Supporting Information

Synthesis, Structure and Spectroscopic Properties of BODIPY Dyes Incorporating the Pentafluorosulfanylphenyl Group

Richard D. James, Fabio Cucinotta, Paul G. Waddell and Andrew C. Benniston

Chemistry-School of Natural and Environmental Sciences, Newcastle University, Newcastle upon Tyne, NE1 7RU, UK.

Table of Contents

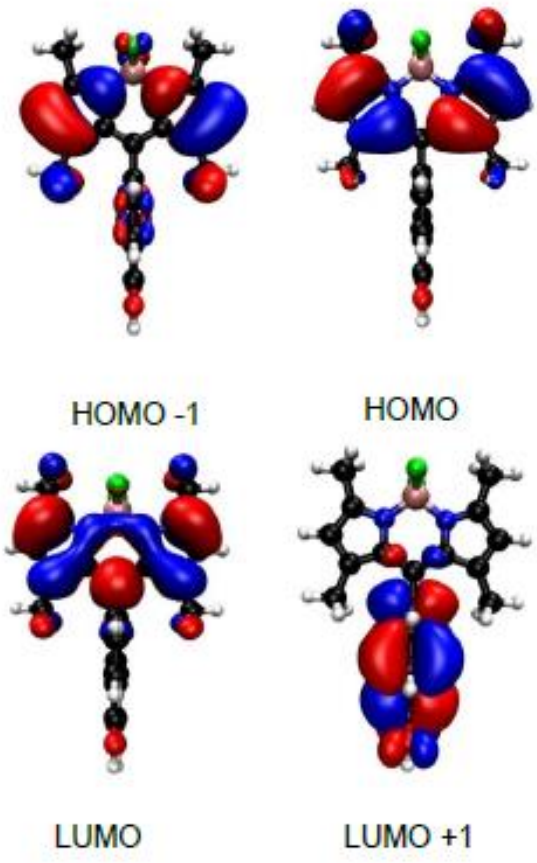

Figure S1. DFT calculated Kohn-Sham molecular orbitals using the B3LYP functional and the 6-311G(d,p) basis set for **BD3.**

Table S1. TD-DFT calculated parameters for the carboxylic acid version of **BD3** in vacuo.

Electronic Transition (oscillator strength)	**Energy / eV (nm)**	**Orbitals**	**% Contribution**
1 (0.6354)	2.85 (434)	HOMO → LUMO	100
2 (0.0498))	3.87 (320)	HOMO-1 → LUMO	100
3 (0.0002)	4.28 (290)	HOMO → LUMO+1	100

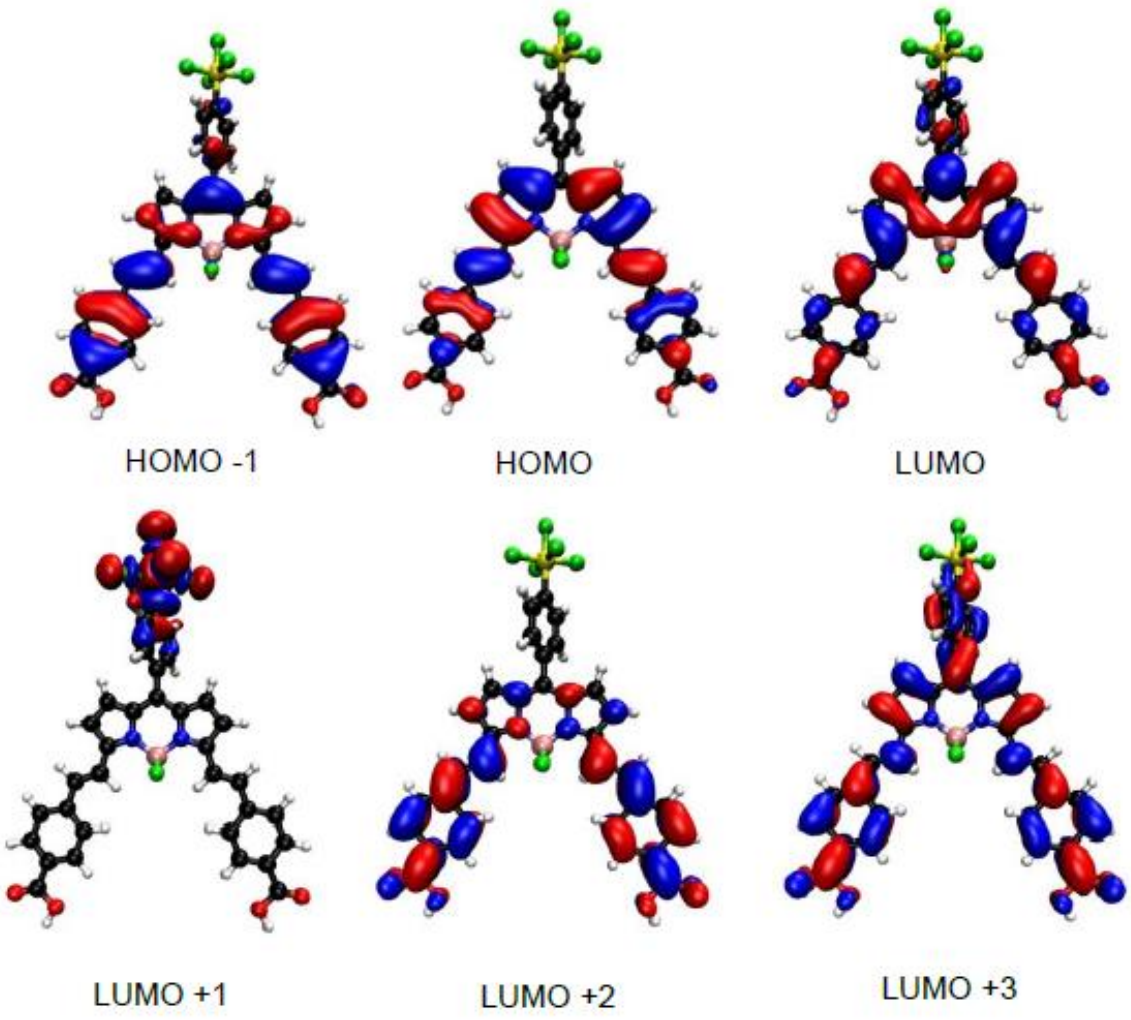

Figure S2. DFT calculated Kohn-Sham molecular orbitals using the B3LYP functional and the 6-311G(d,p) basis set for **BD4.**

Table S2. TD-DFT calculated parameters for the carboxylic acid version of **BD4** in vacuo.

Electronic Transition (oscillator strength)	**Energy / eV (nm)**	**Orbitals**	**% Contribution**
1 (1.1086)	2.12 (586)	HOMO → LUMO	100
2 (2.1656)	3.54 (351)	HOMO-1 → LUMO HOMO → LUMO+2	79 21
3 (0.1365)	3.67 (338)	HOMO → LUMO+2 HOMO-1 → LUMO HOMO-1 → LUMO+3	74 22 4

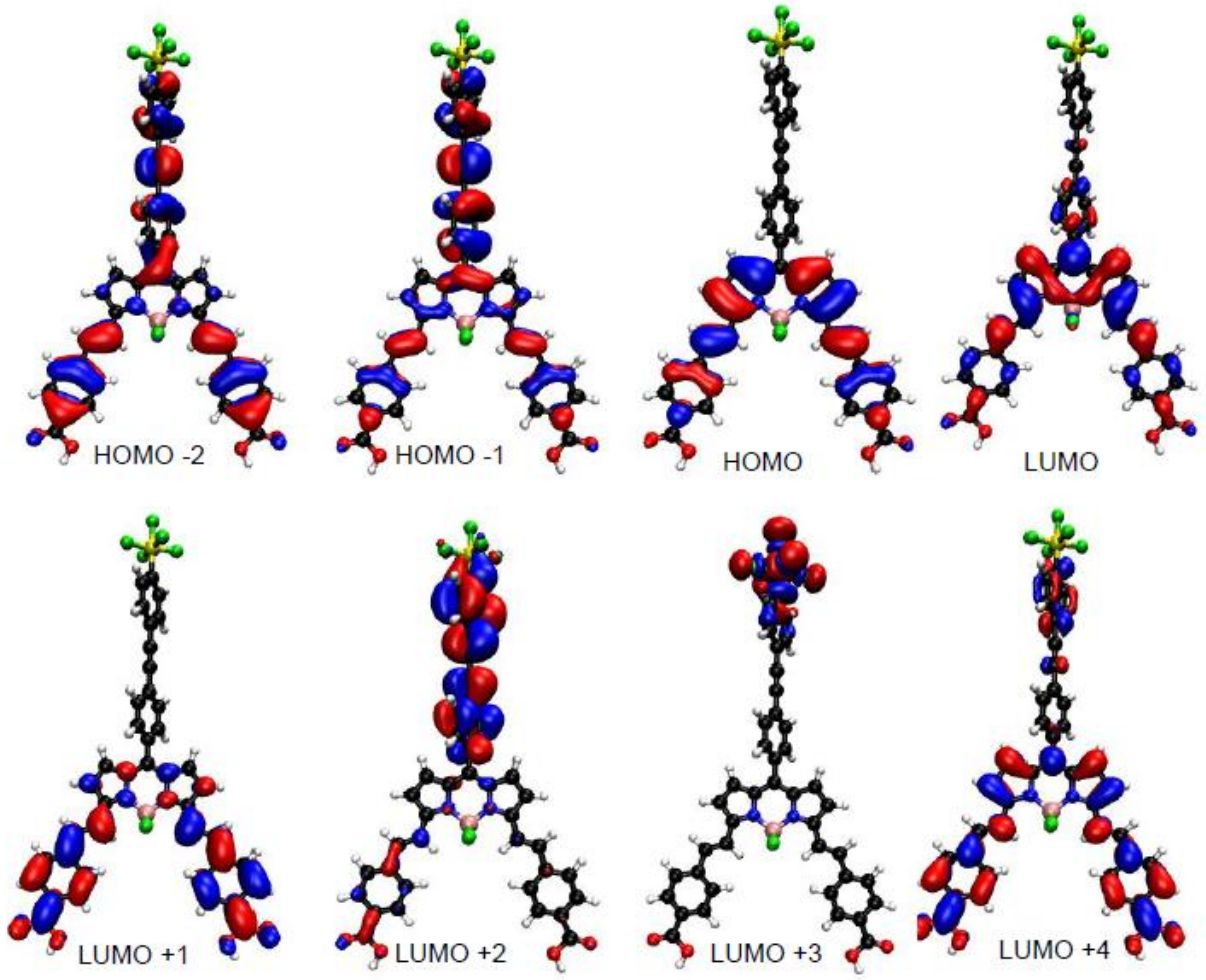

Figure S3. DFT calculated Kohn-Sham molecular orbitals using the B3LYP functional and the 6-311G(d,p) basis set for **BD5.**

Table S3. TD-DFT calculated parameters for the carboxylic acid version of **BD5** in vacuo.

Electronic Transition (oscillator strength)	**Energy / eV (nm)**	**Orbitals**	**% Contribution**
1 (1.0604)	2.23 (556)	HOMO → LUMO	100
2 (2.2145)	3.40 (365)	HOMO-1 → LUMO HOMO→ LUMO+1 HOMO-2 → LUMO HOMO-2 → LUMO+2 HOMO-1 → LUMO+2	86 5 3 3 3
3 (0.5933)	3.79 (327)	HOMO → LUMO+1 HOMO-1 → LUMO HOMO-1 → LUMO+4 HOMO-2 → LUMO+4	89 5 3 2

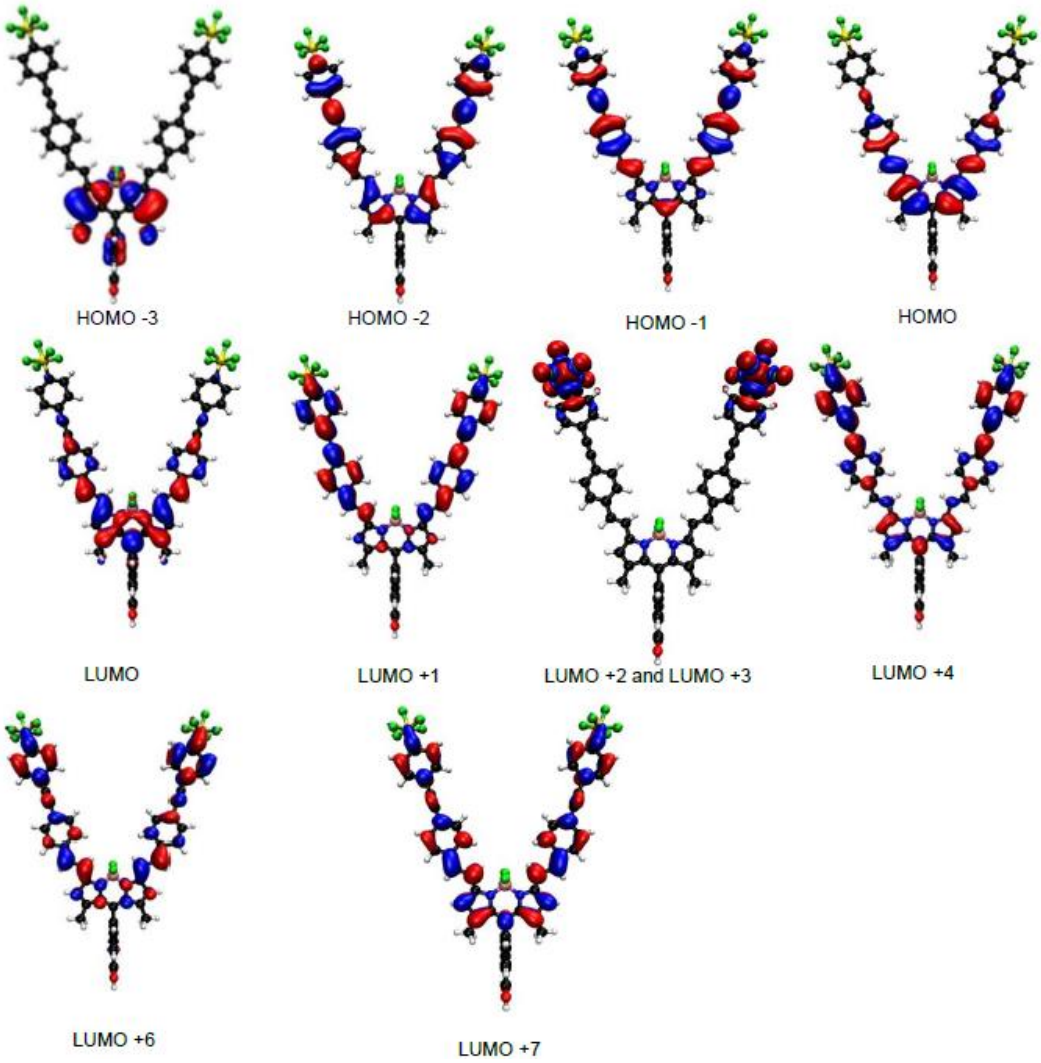

Figure S4. DFT calculated Kohn-Sham molecular orbitals using the B3LYP functional and the 6-311G(d,p) basis set for **BD6.**

Table S4. TD-DFT calculated parameters for the carboxylic acid version of **BD6** in vacuo.

Electronic Transition (oscillator strength)	**Energy / eV (nm)**	**Orbitals**	**% Contribution**
1 (1.2547)	2.07 (599)	HOMO→LUMO HOMO-1→LUMO+1	97 3
2 (3.8114)	3.31 (375)	HOMO-1→LUMO HOMO→LUMO+1 HOMO-2→LUMO+1 HOMO-1→LUMO+4 HOMO→LUMO+6	47 40 5 4 4
3 (0.0999)	3.64 (341)	HOMO-3→LUMO HOMO→LUMO+4 HOMO-2→LUMO HOMO-1→LUMO+1 HOMO-1→LUMO+7	41 26 16 12 5

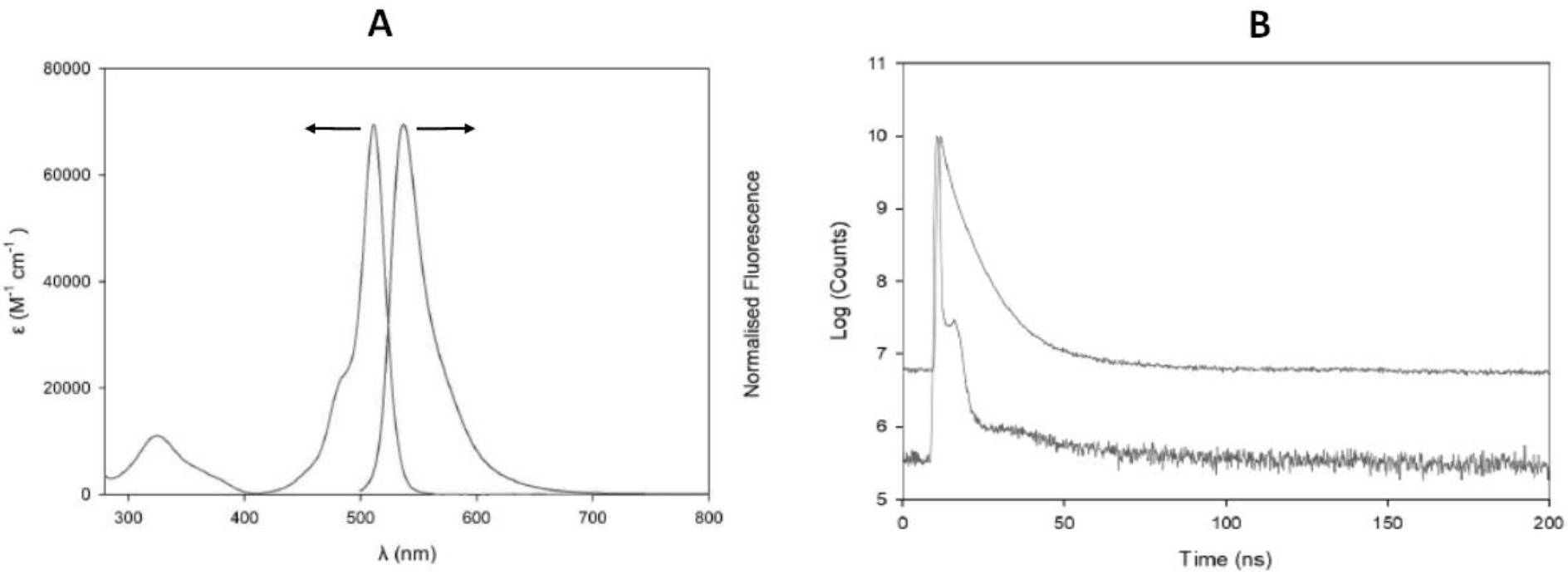

Figure S5. (A) Absorption and emission spectra recorded for **BD1** in CH_3CN at room temperature. (B) Fluorescence decay trace (top) and instrument response function (bottom) measured for **BD1** in CH_3CN using single-photon-counting.

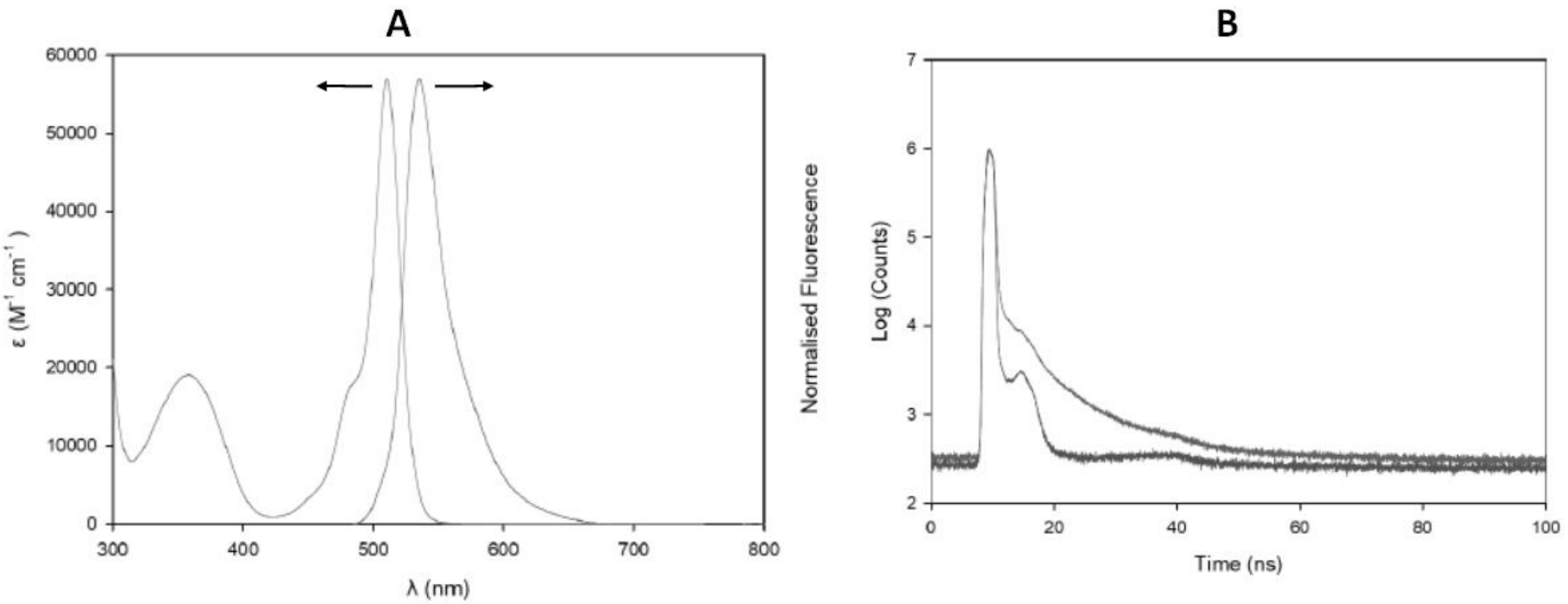

Figure S6. (A) Absorption and emission spectra recorded for **BD2** in CH_3CN at room temperature. (B) Fluorescence decay trace (top) and instrument response function (bottom) measured for **BD2** in CH_3CN using single-photon-counting.

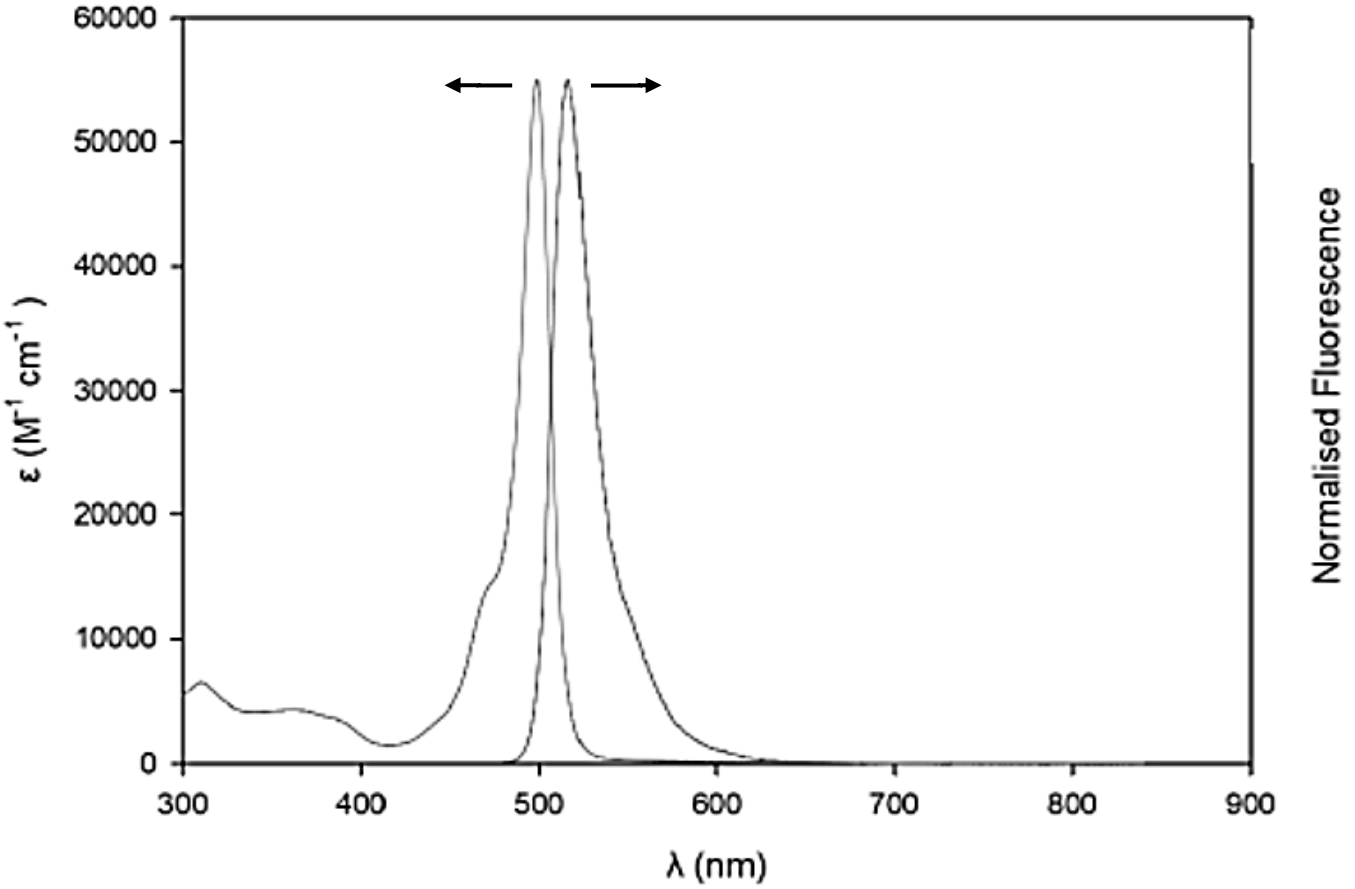

Figure S7. Absorption and emission spectra recorded for **BD3** in CH_3CN at room temperature.

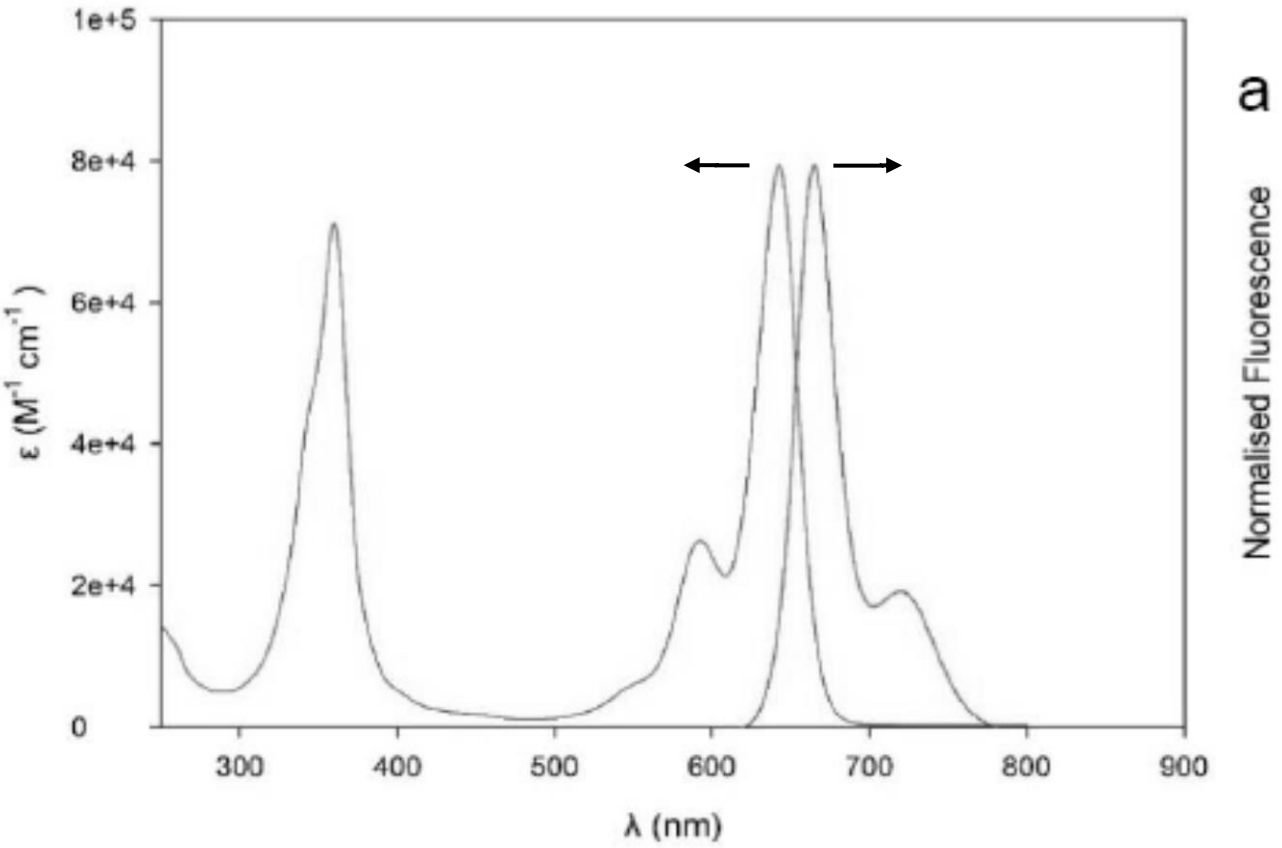

Figure S8. Absorption and emission spectra recorded for **BD4** in CH_3CN at room temperature.

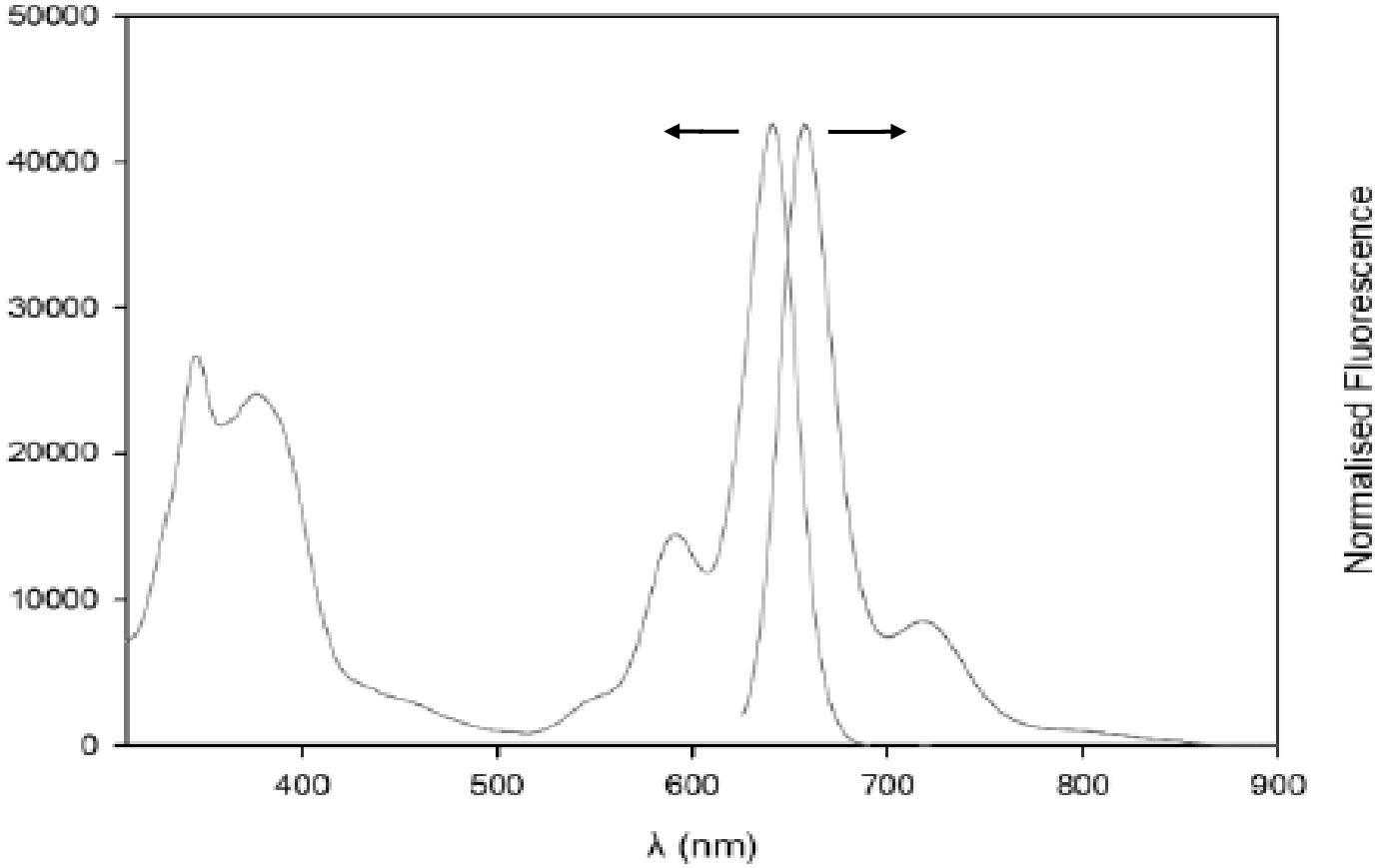

Figure S9. Absorption and emission spectra recorded for **BD5** in CH_3CN at room temperature.

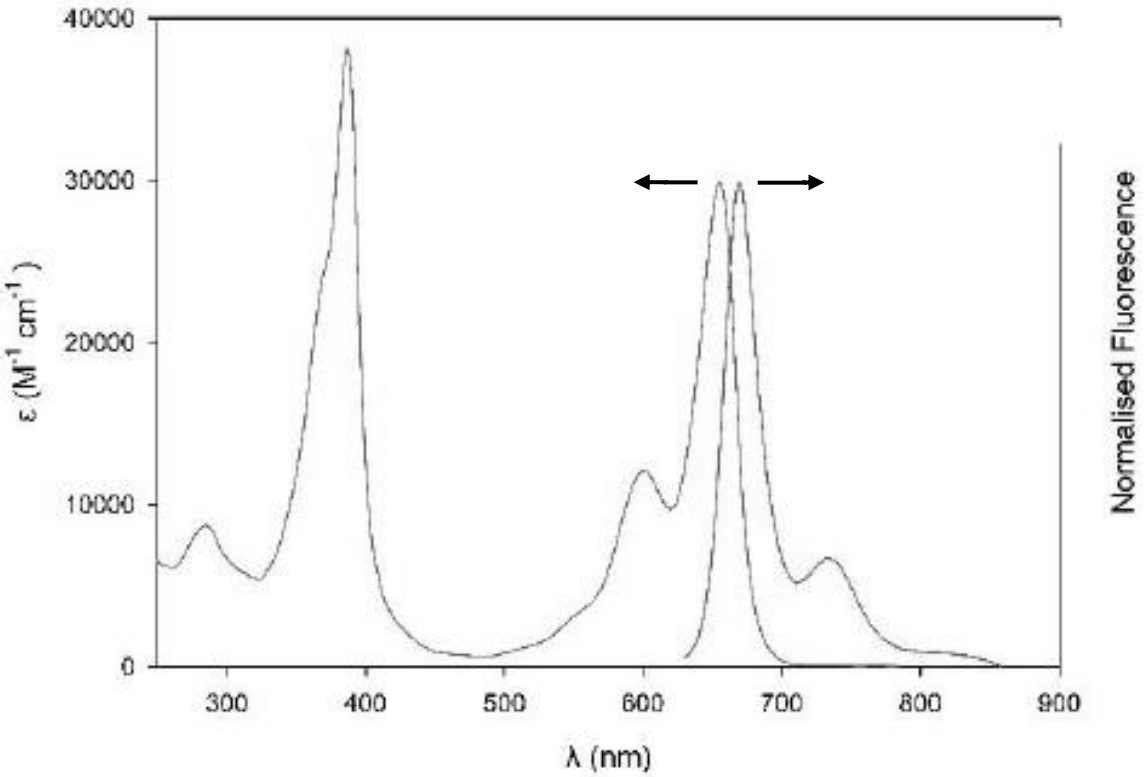

Figure S10. Absorption and emission spectra recorded for **BD6** in CH_3CN at room temperature.

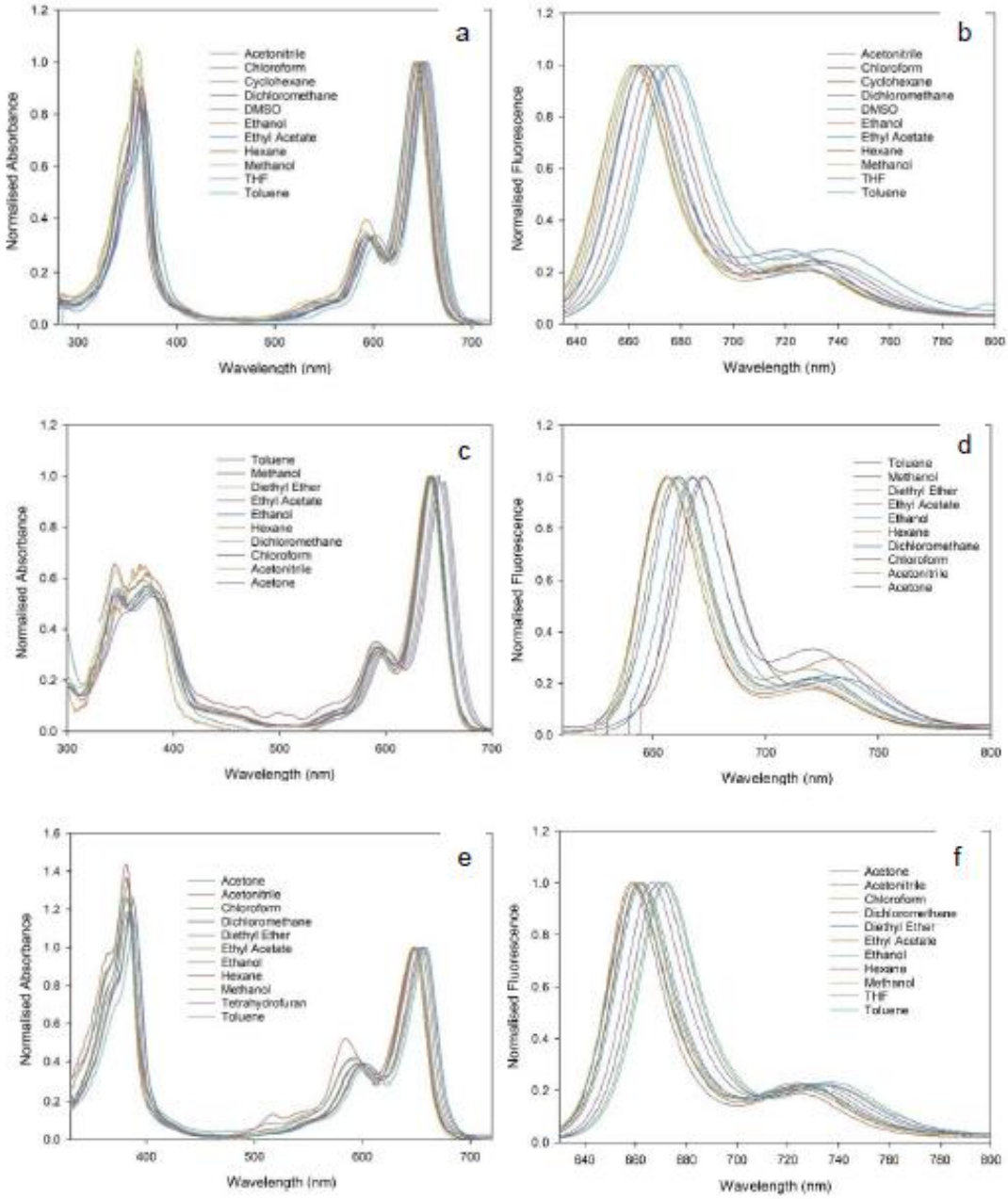

Figure S11. Absorption and emission spectra recorded for **BD4** (a and b), **BD5** (c and d) and **BD6** (e and f) in a range of solvents at room temperature.

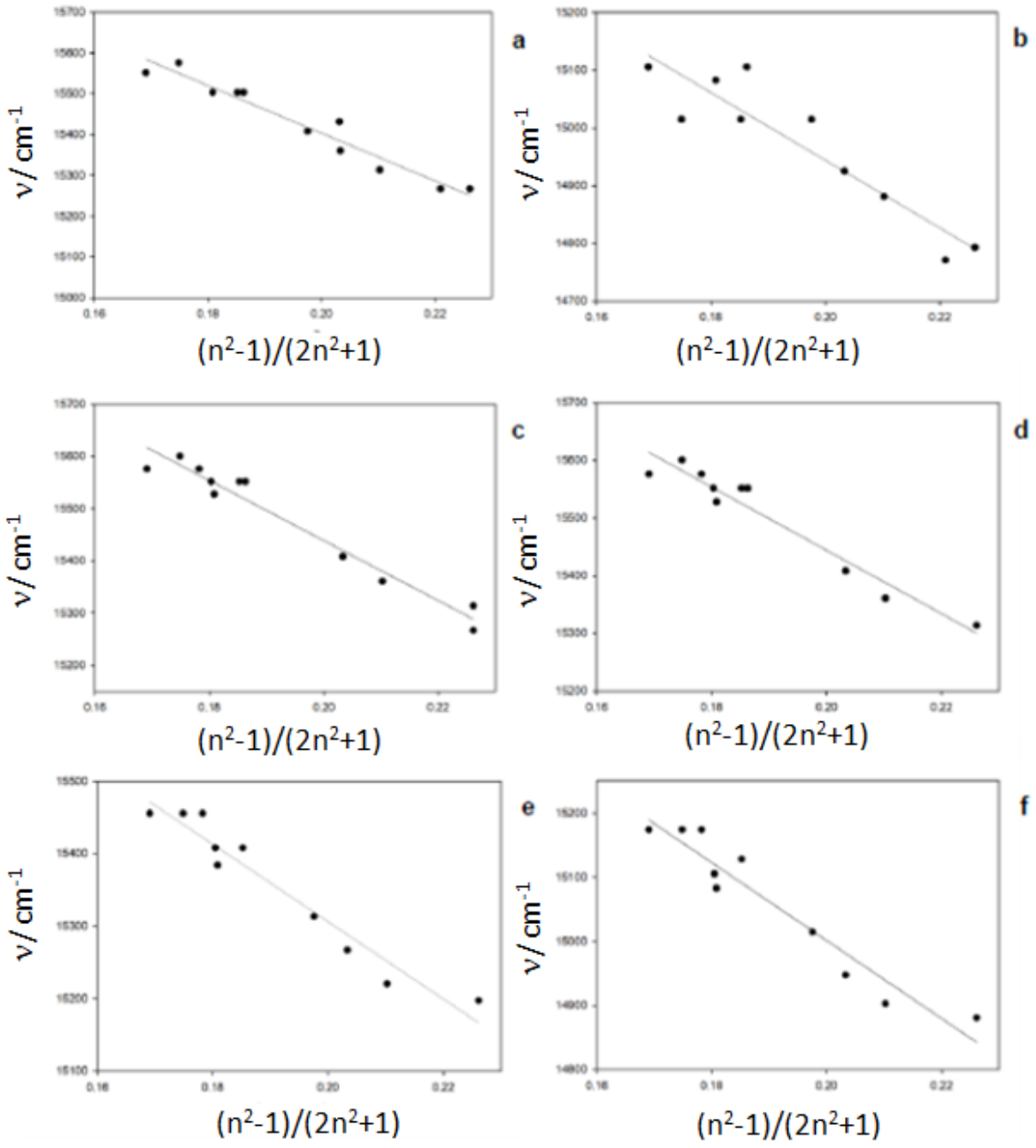

Figure S12. Plots of absorption maxima and emission maxima versus the solvent polarizability function for **BD4** (a and b), **BD5** (c and d) and **BD6** (e and f).

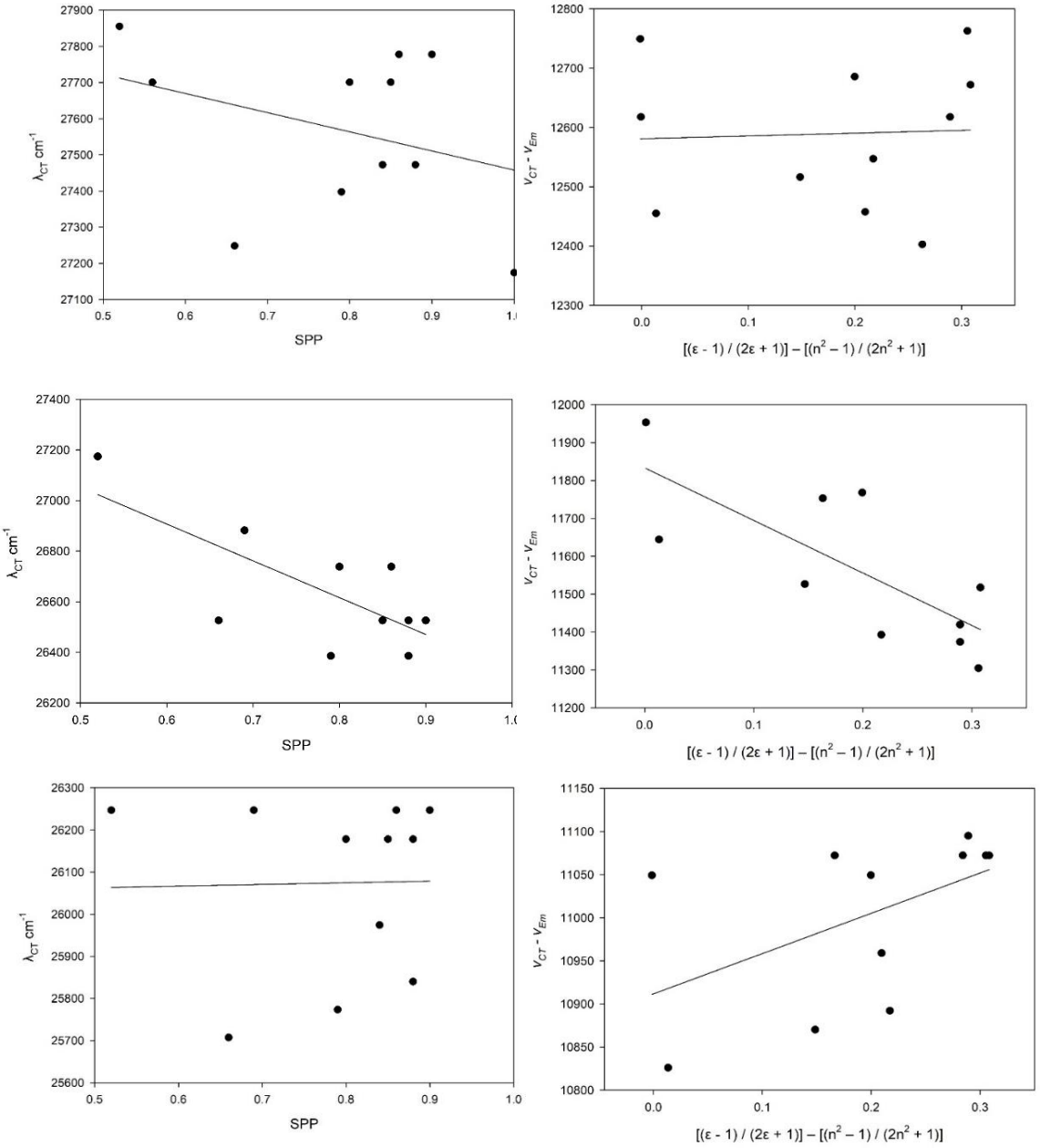

Figure S13. Catalán's Solvent Polarity (SPP) and Lippert Mataga plots for **BD4** (top), **BD5** (middle) and **BD6** (bottom).

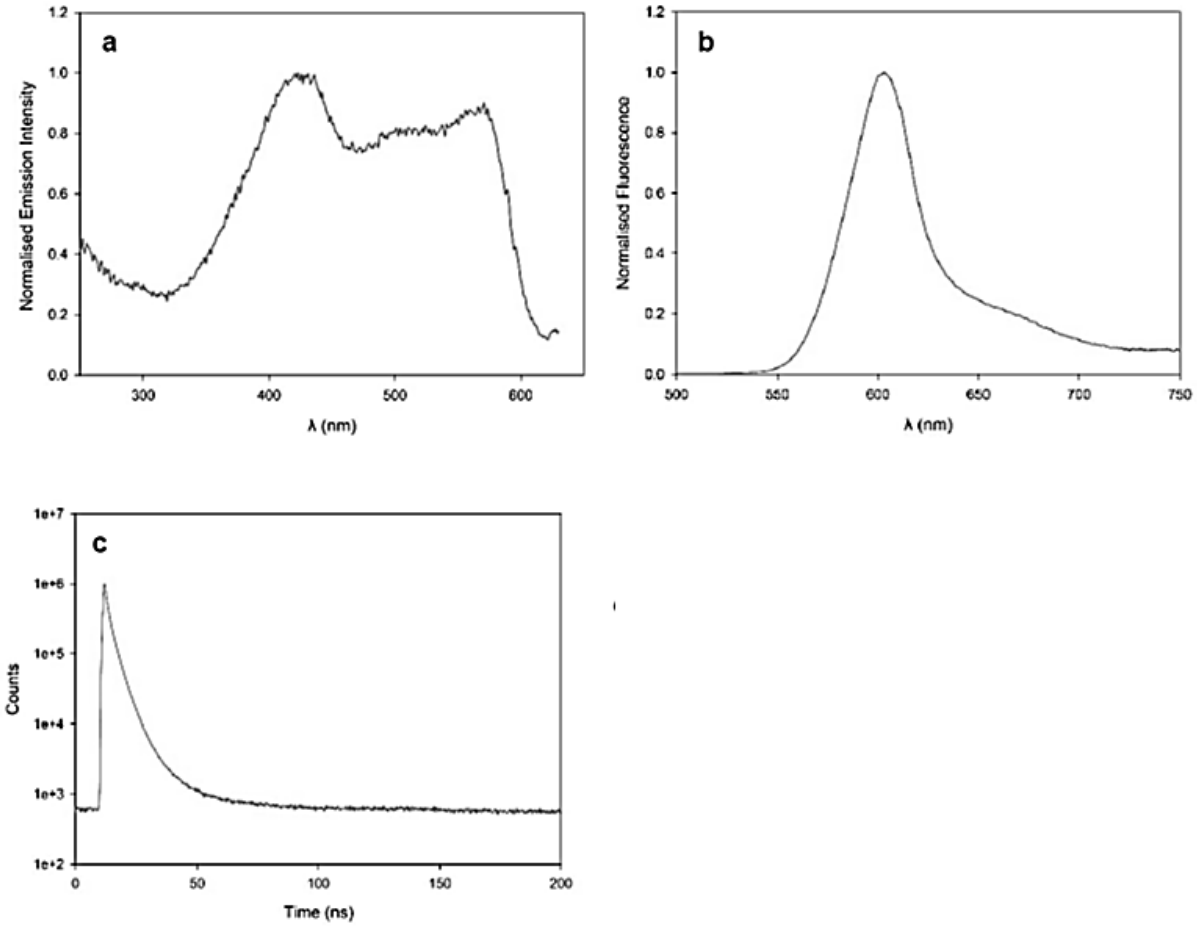

Figure S14. (a) Excitation spectrum measured at 650 nm, (b) fluorescence spectrum using 480 nm excitation and (c) fluorescence lifetime decay for a crystalline sample of **BD1.**

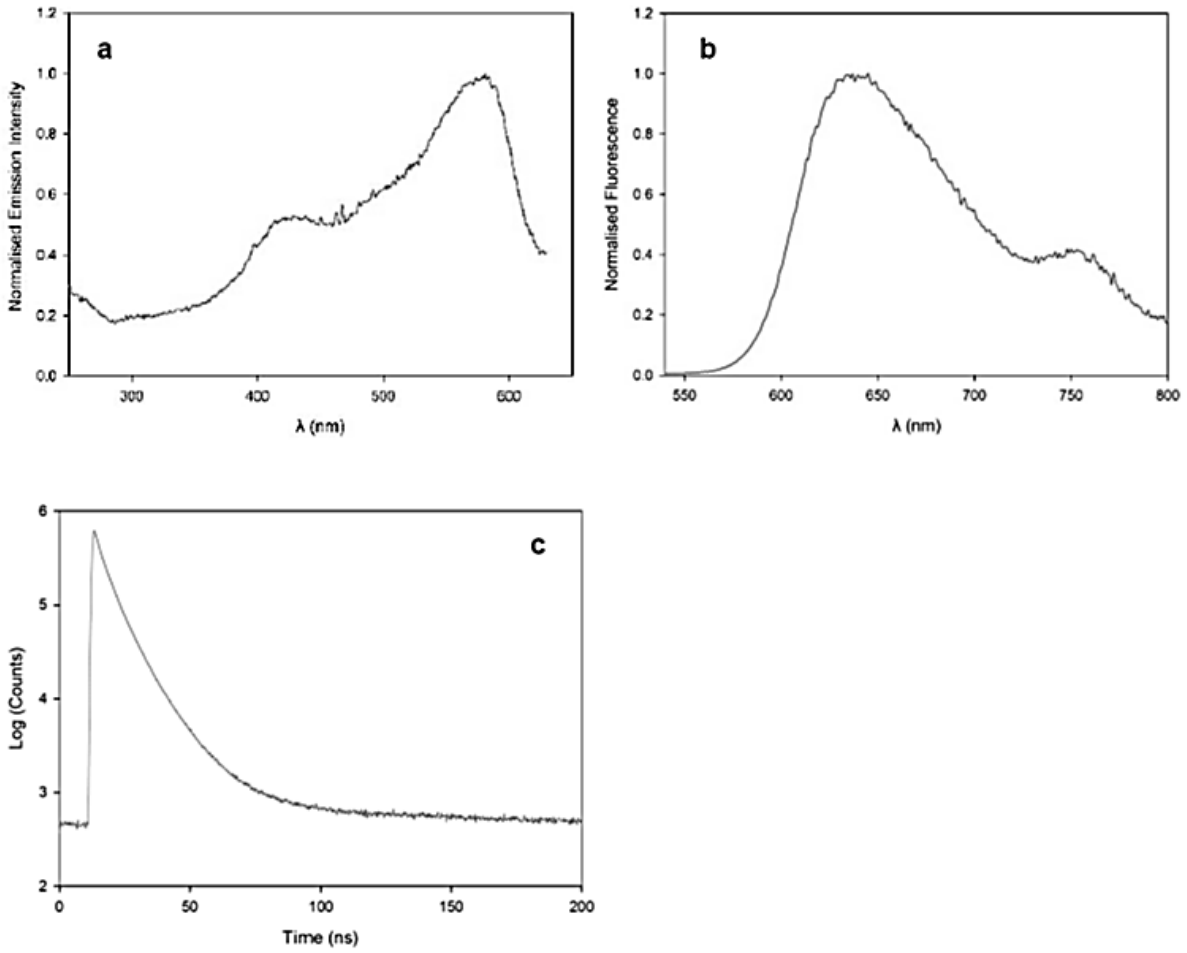

Figure S15. (a) Excitation spectrum measured at 630 nm, (b) fluorescence spectrum using 400 nm excitation and (c) fluorescence lifetime decay for a crystalline sample of **BD2.**

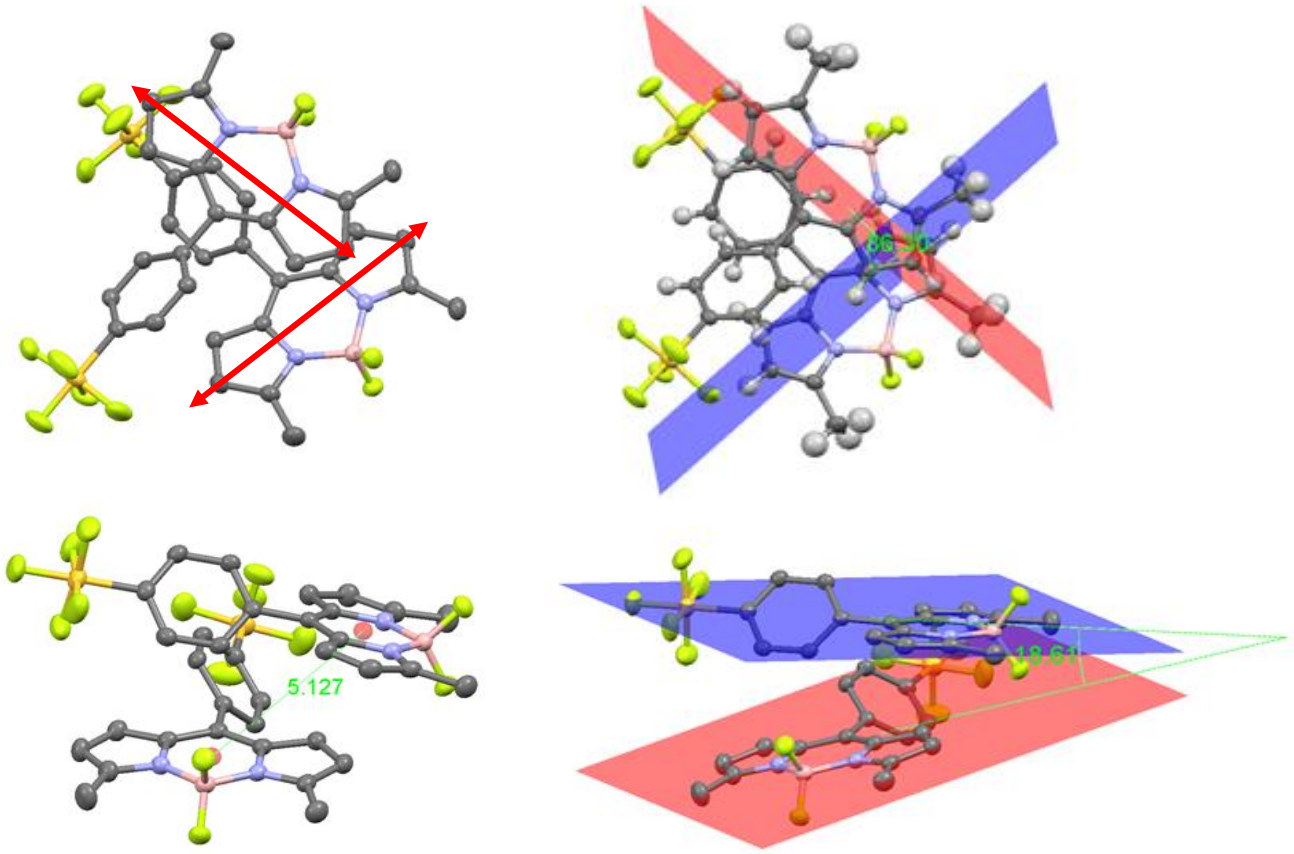

Figure S16. Representation of planes, angles and distances with regard to the electronic transition dipoles (red) for **BD1** as obtained from the crystal packing diagram.

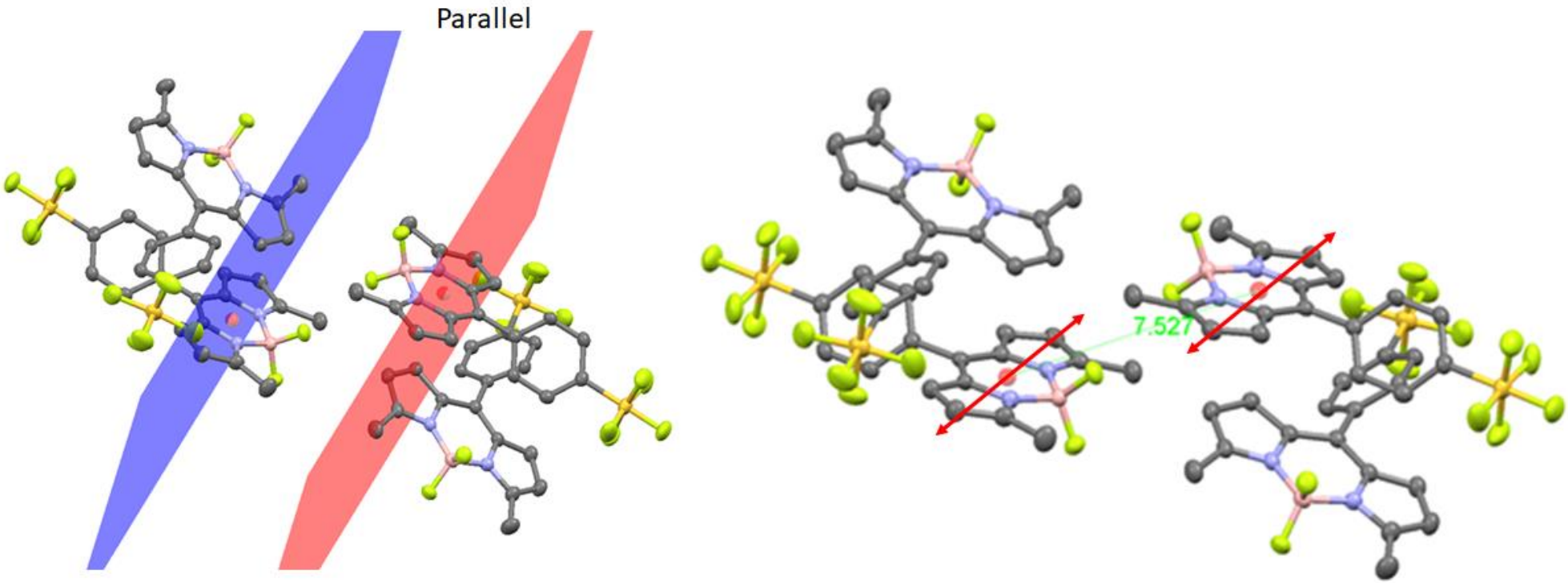

Figure S17. Representation of a dimer for **BD1** and separation distance as obtained from the crystal packing diagram.

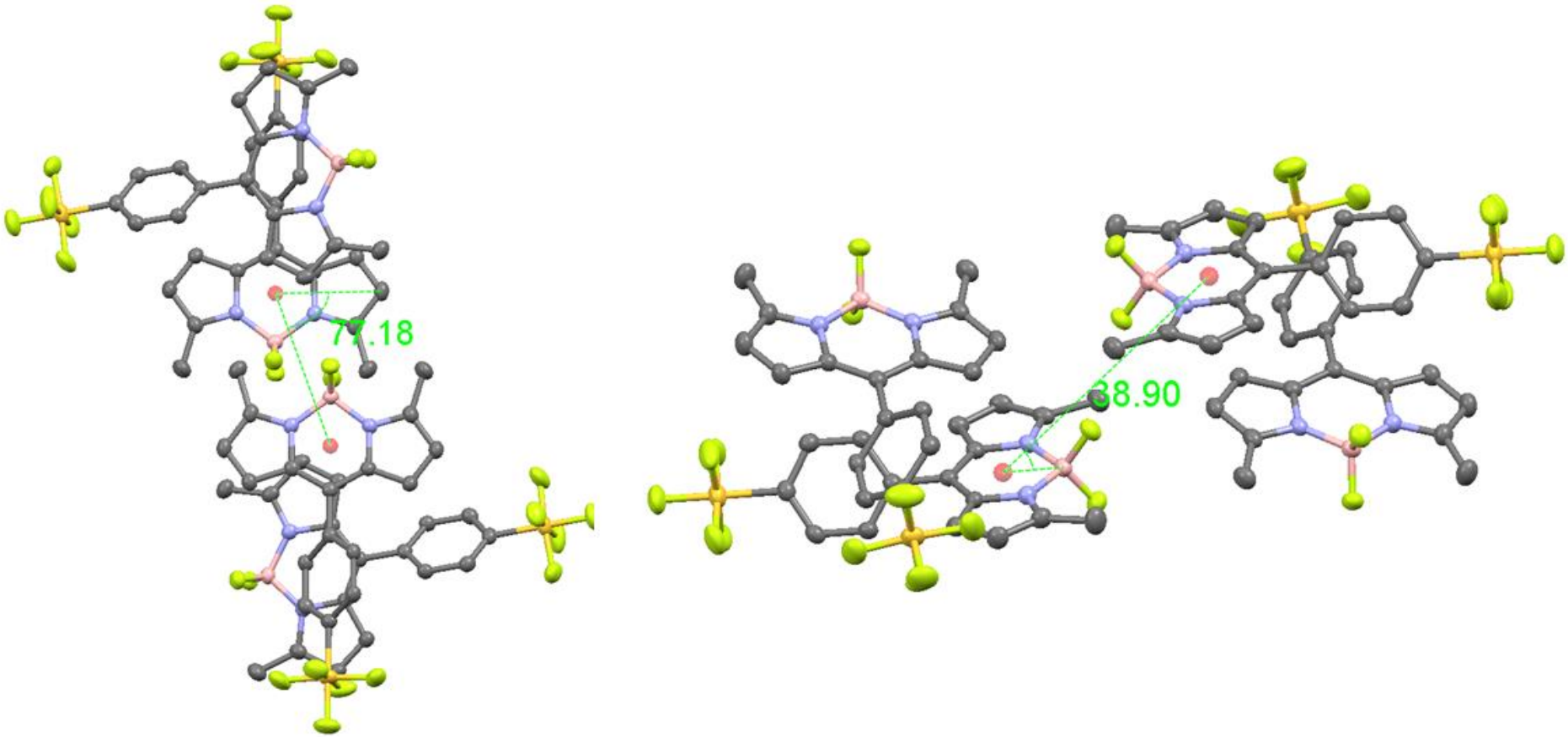

Figure S18. Representation of an offset face-to-face dimer for **BD1** and separation distance as obtained from the crystal packing diagram.

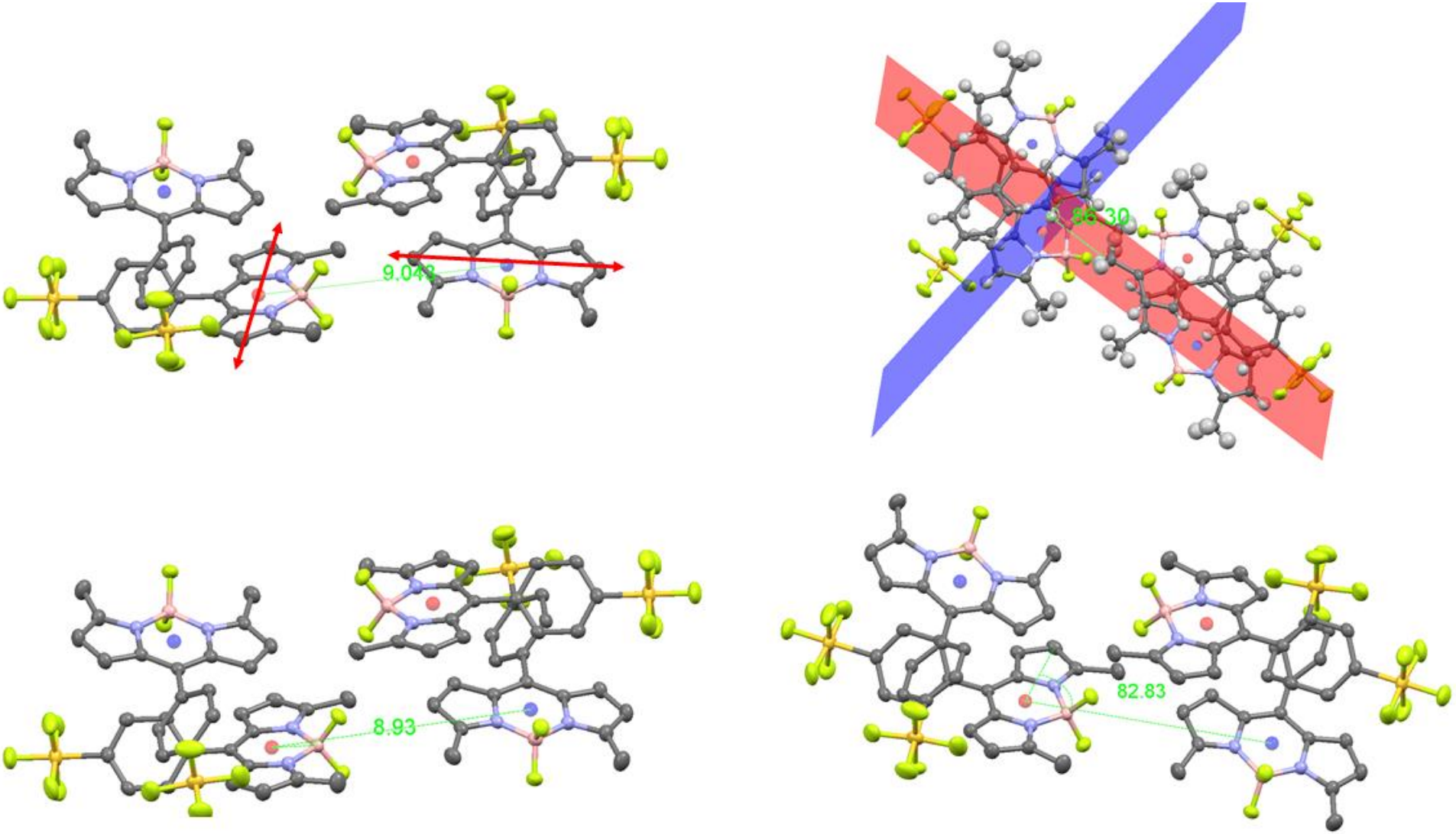

Figure S19. Representation of a dimer for **BD1** between separate stacks and the separation distance and angles as obtained from the crystal packing diagram.

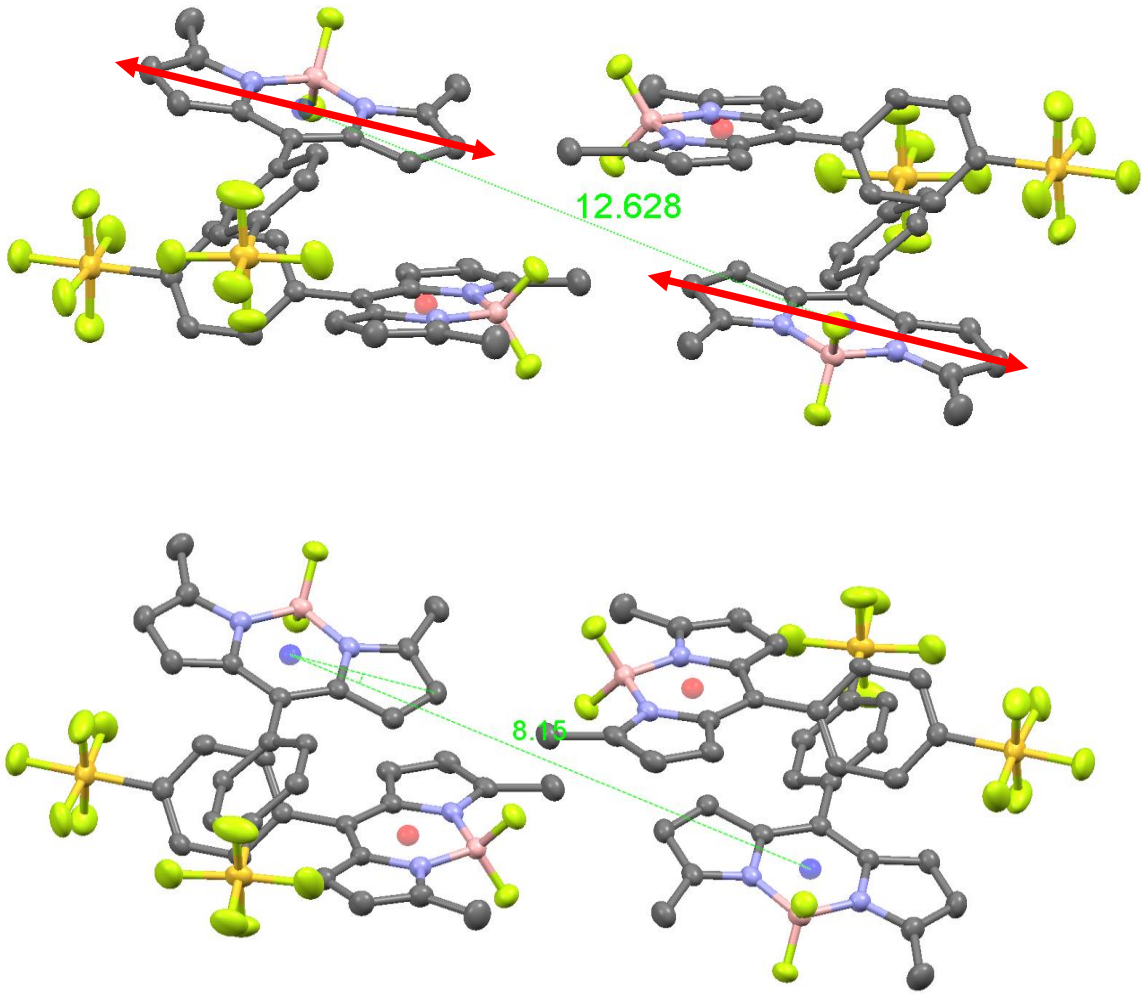

Figure S20. Representation of an offset co-linear dimer for **BD1** and separation distance and offset angle as obtained from the crystal packing diagram.

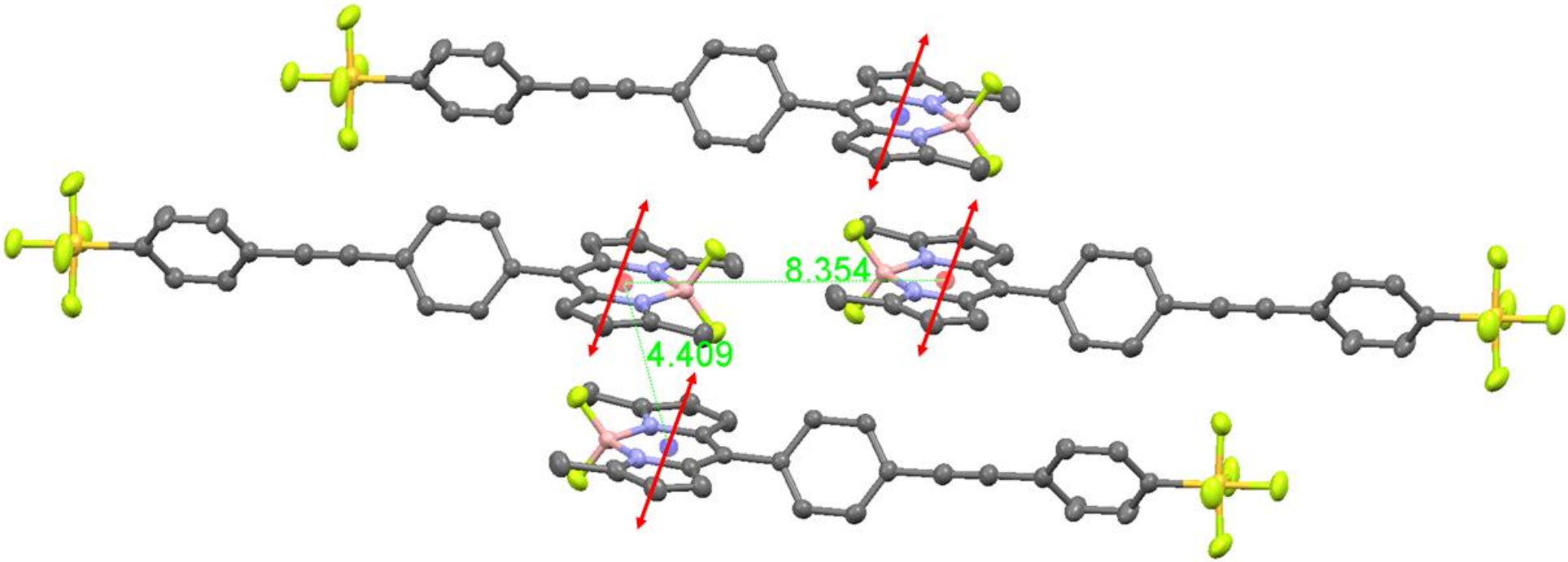

Figure S21. Representation of dimers for **BD2** and separation distance as obtained from the crystal packing diagram.

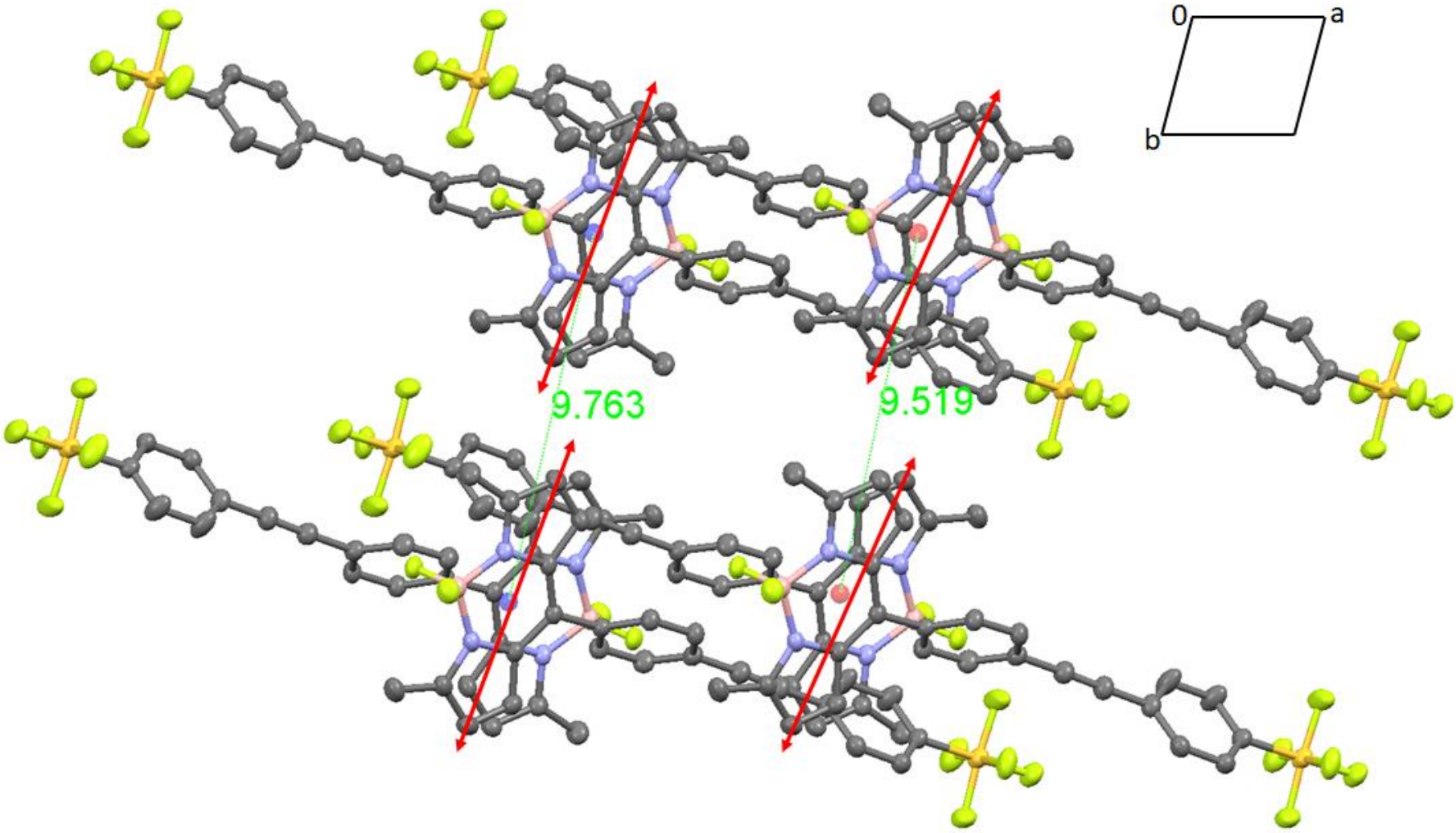

Figure S22. Representation of pseudo co-linear dimers for **BD2** and their separation distances as obtained from the crystal packing diagram. View is down the c-axis.

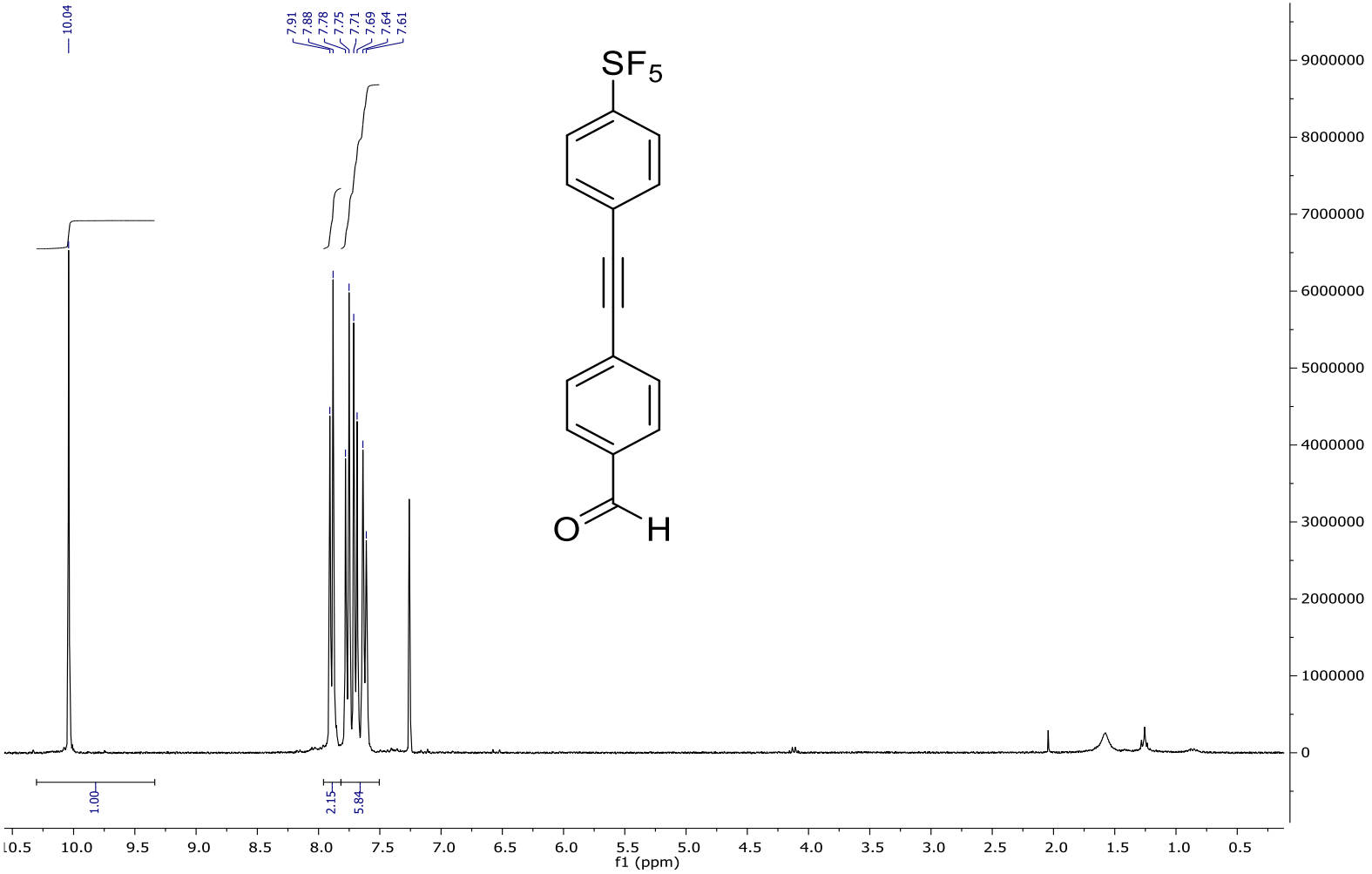

Figure S23. A 300 MHz ^{1}H NMR spectrum of **2** recorded in $CDCl_3$.

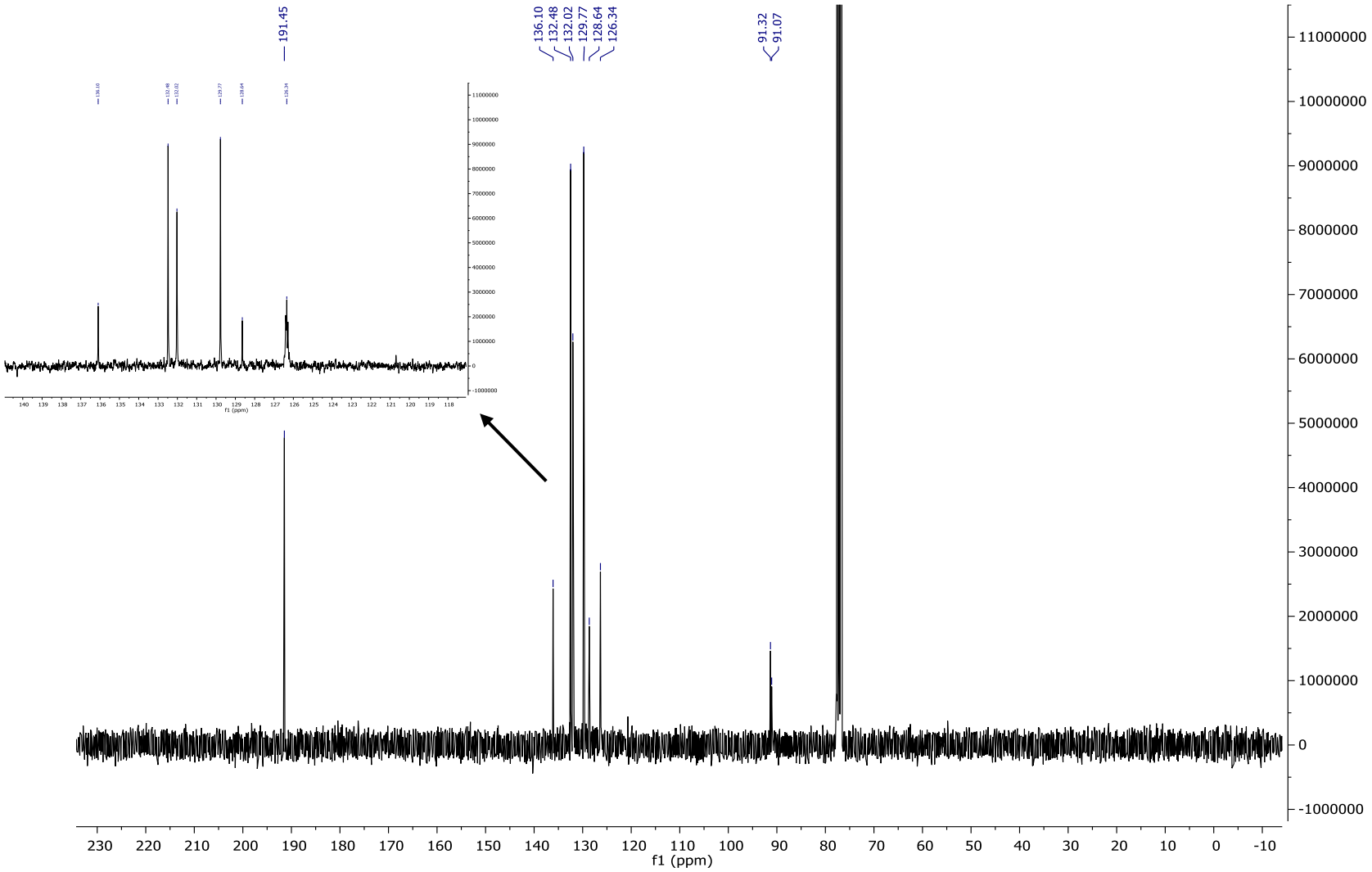

Figure S24. A 176 MHz $^{13}C\{^{1}H\}$ NMR spectrum of **2** recorded in $CDCl_3$.

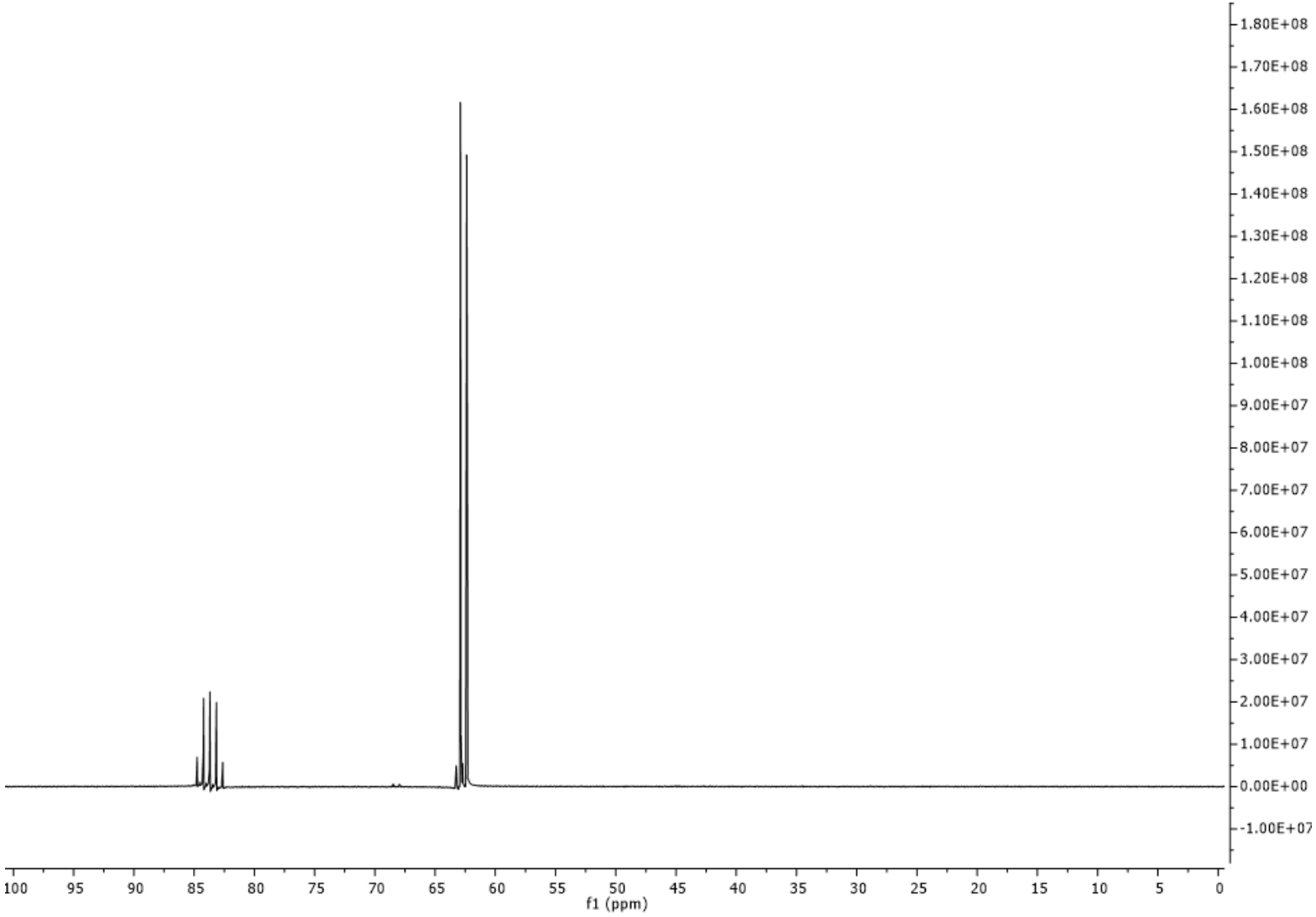

Figure S25. A 282 MHz ^{19}F NMR spectrum of **2** recorded in $CDCl_3$.

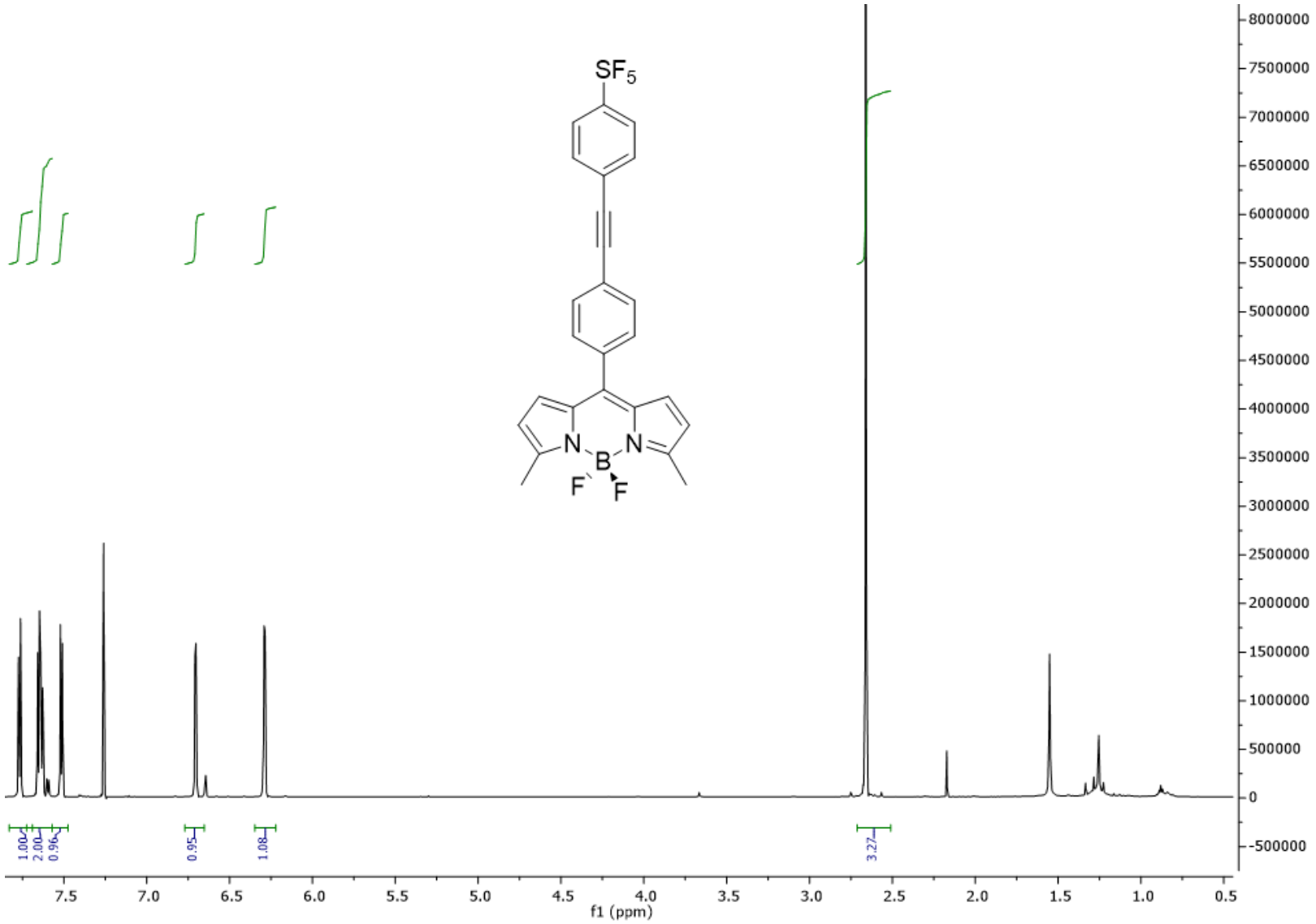

Figure S26. A 700 MHz ^{1}H NMR spectrum of **BD2** recorded in $CDCl_3$.

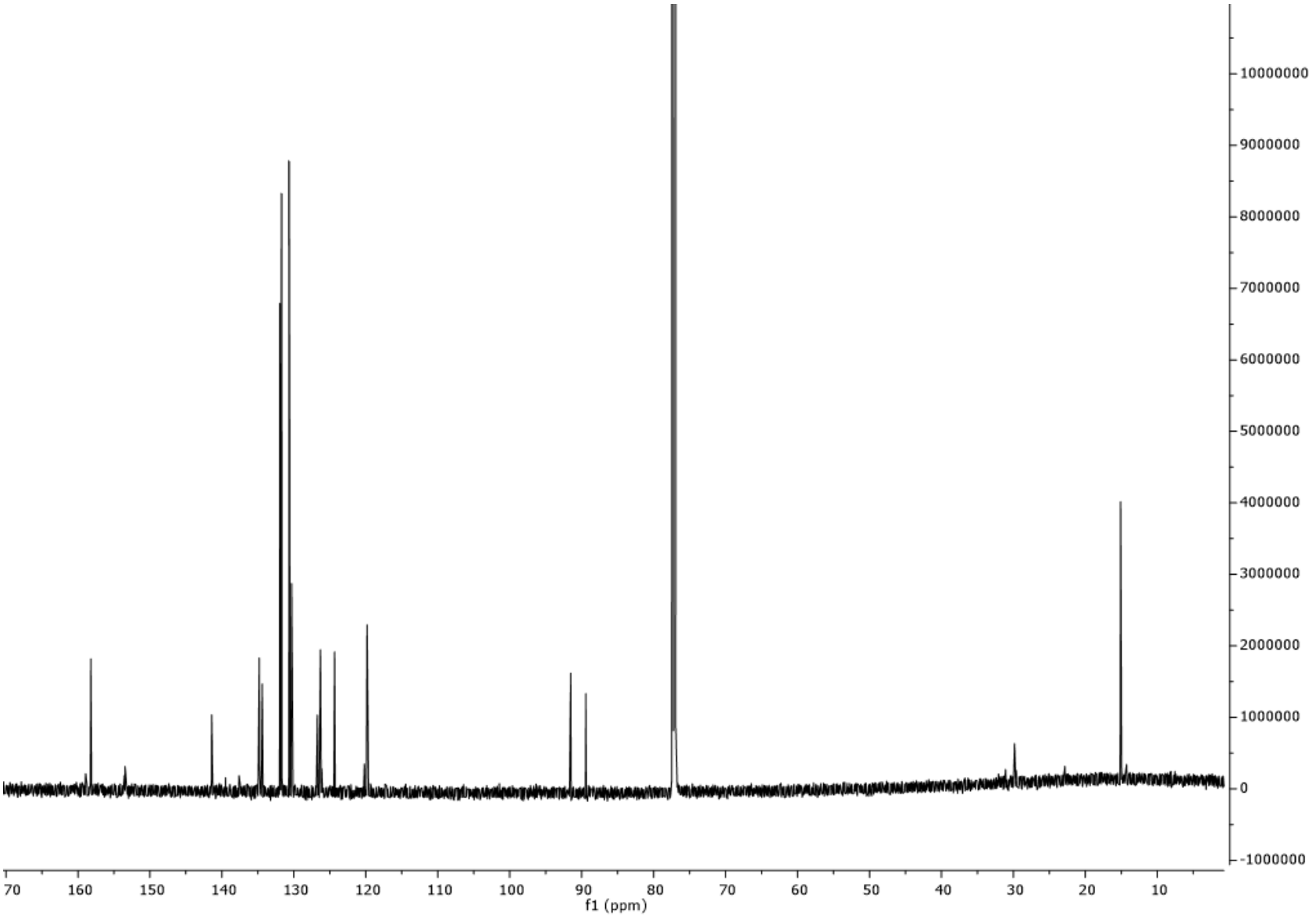

Figure S27. A 176 MHz $^{13}C\{^{1}H\}$ NMR spectrum of **BD2** recorded in $CDCl_3$.

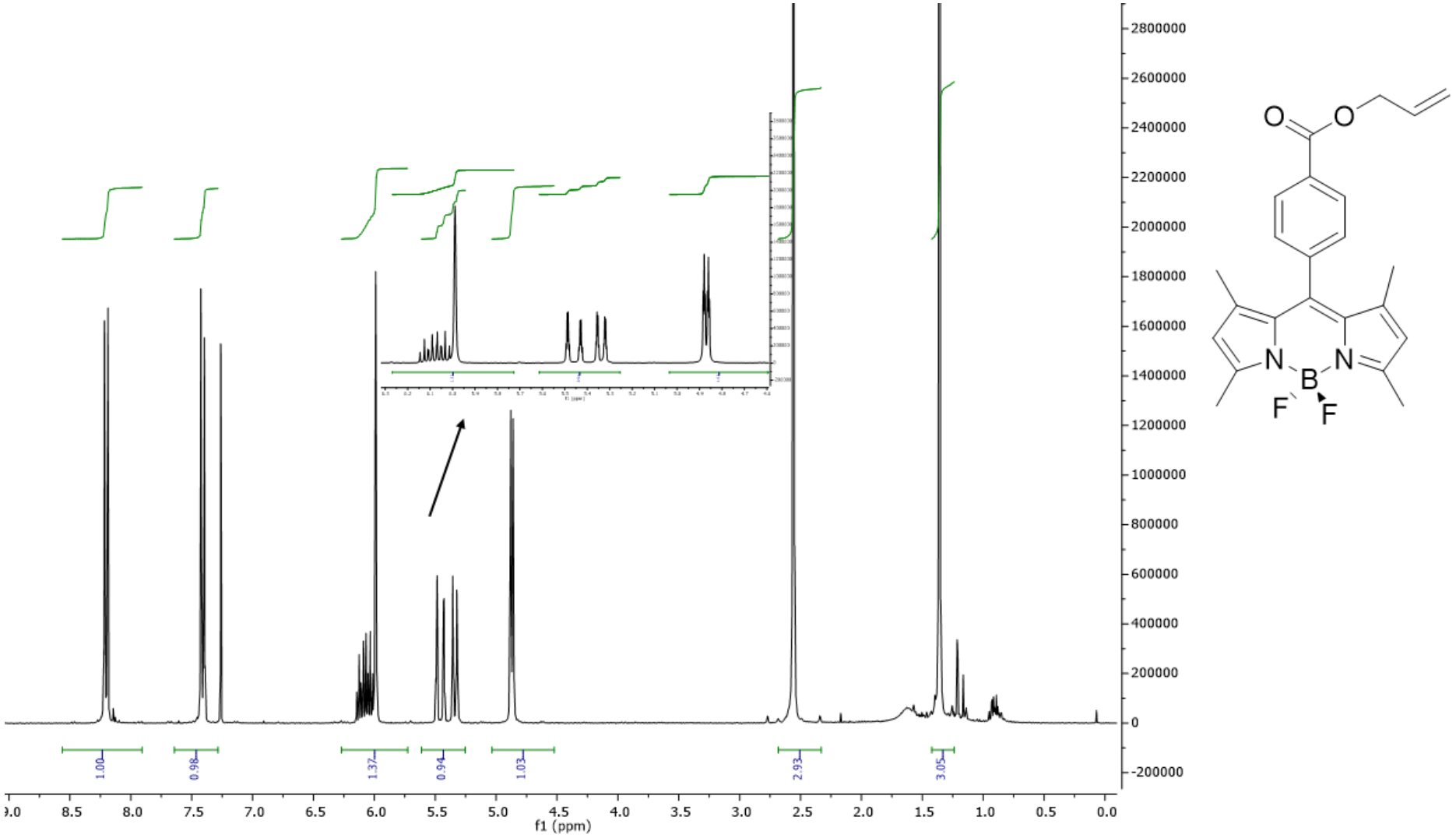

Figure S28. A 300 MHz ^{1}H NMR spectrum of **BD3** recorded in $CDCl_3$.

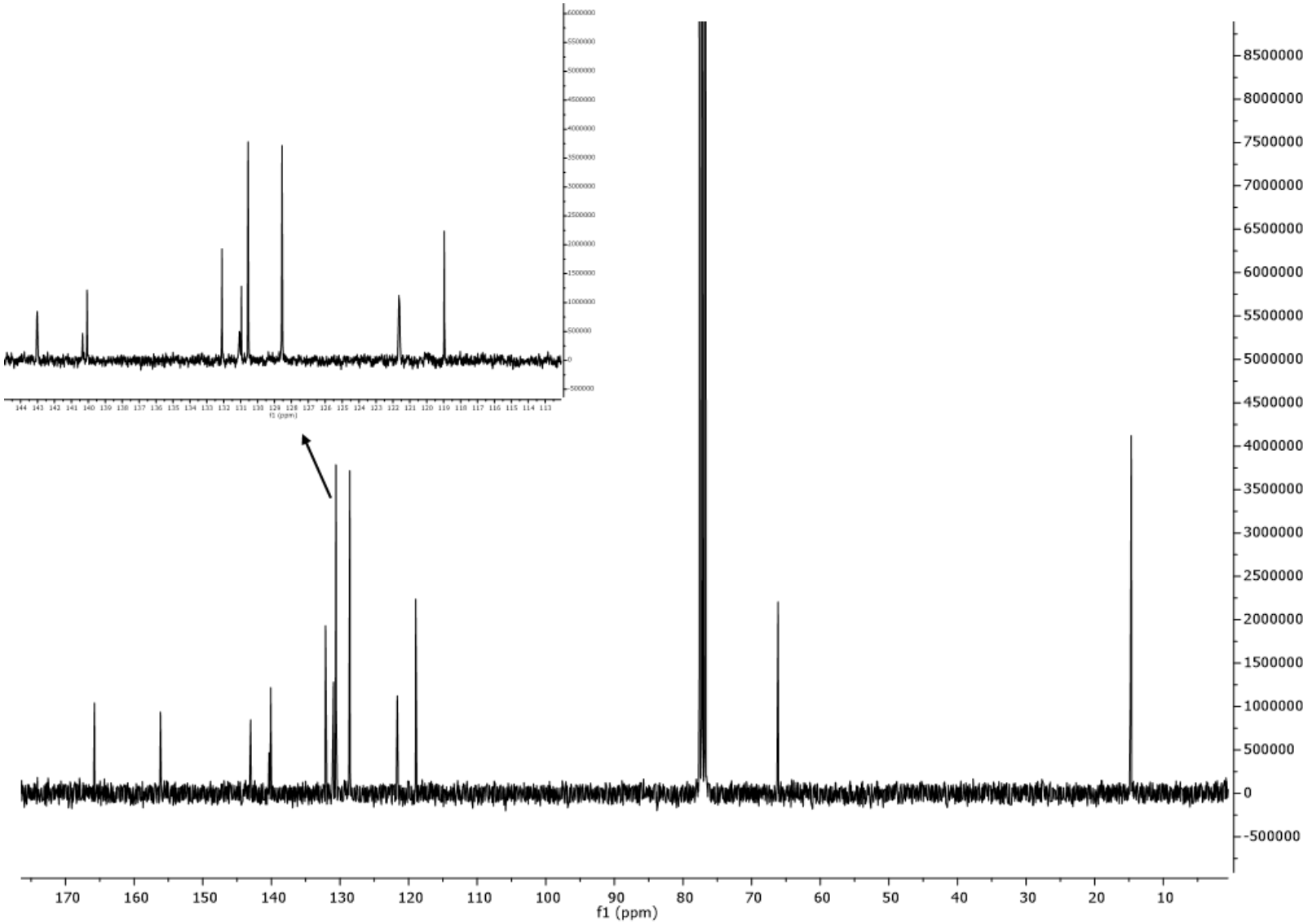

Figure S29. A 75 MHz $^{13}C\{^{1}H\}$ NMR spectrum of **BD3** recorded in $CDCl_3$.

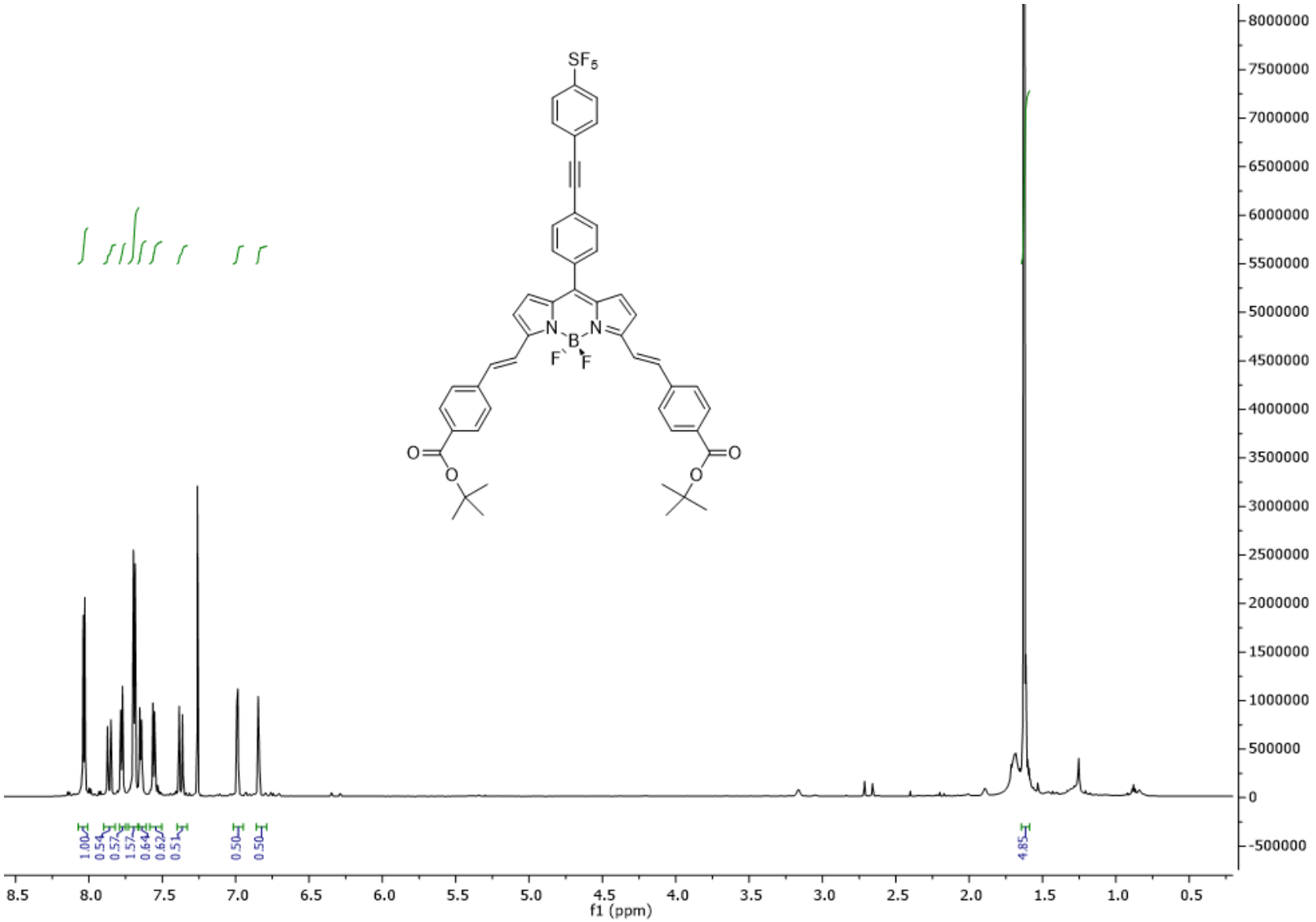

Figure S30. A 700 MHz ^{1}H NMR spectrum of **BD5** recorded in $CDCl_3$.

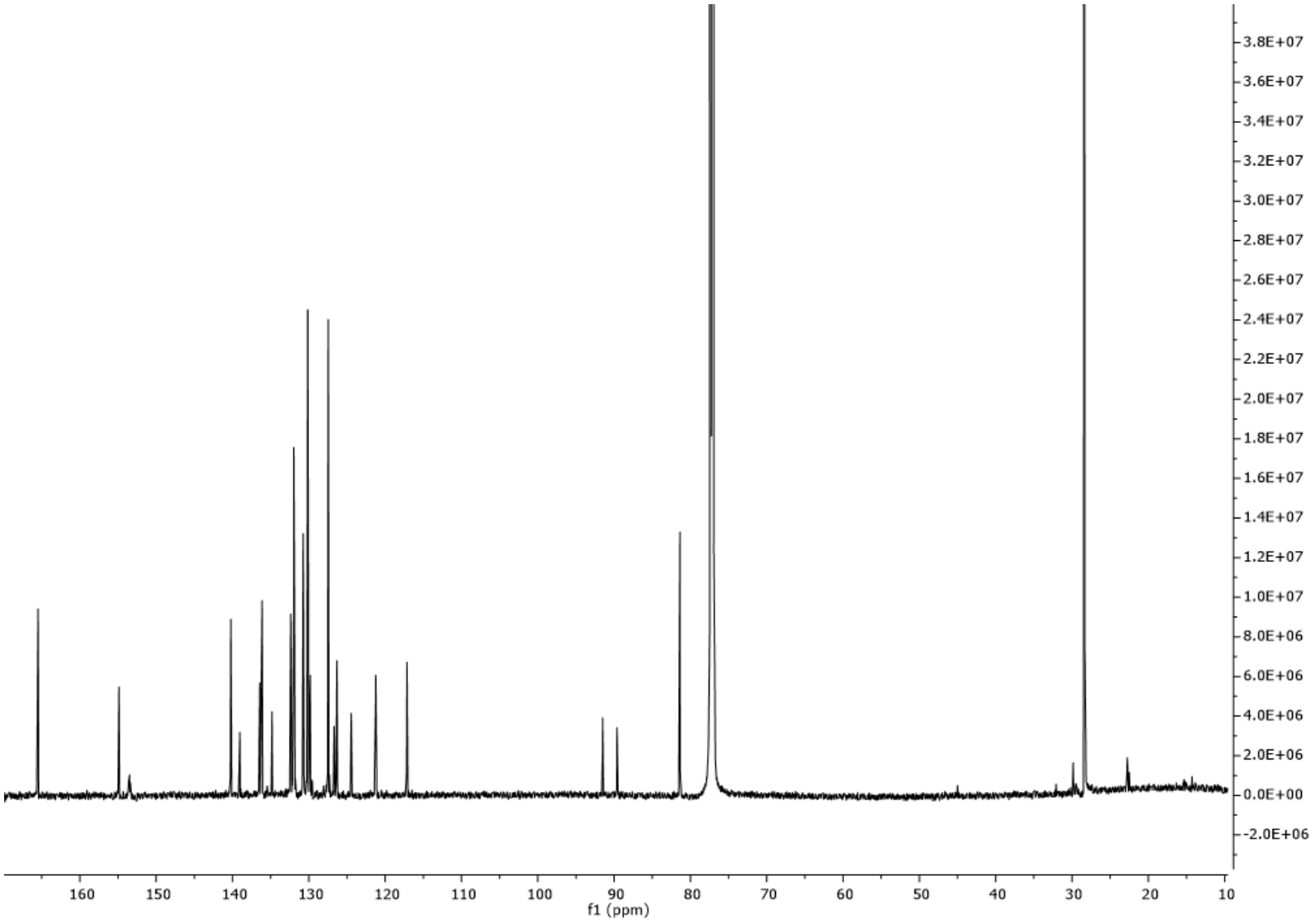

Figure S31. A 176 MHz $^{13}C\{^{1}H\}$ NMR spectrum of **BD5** recorded in $CDCl_3$.

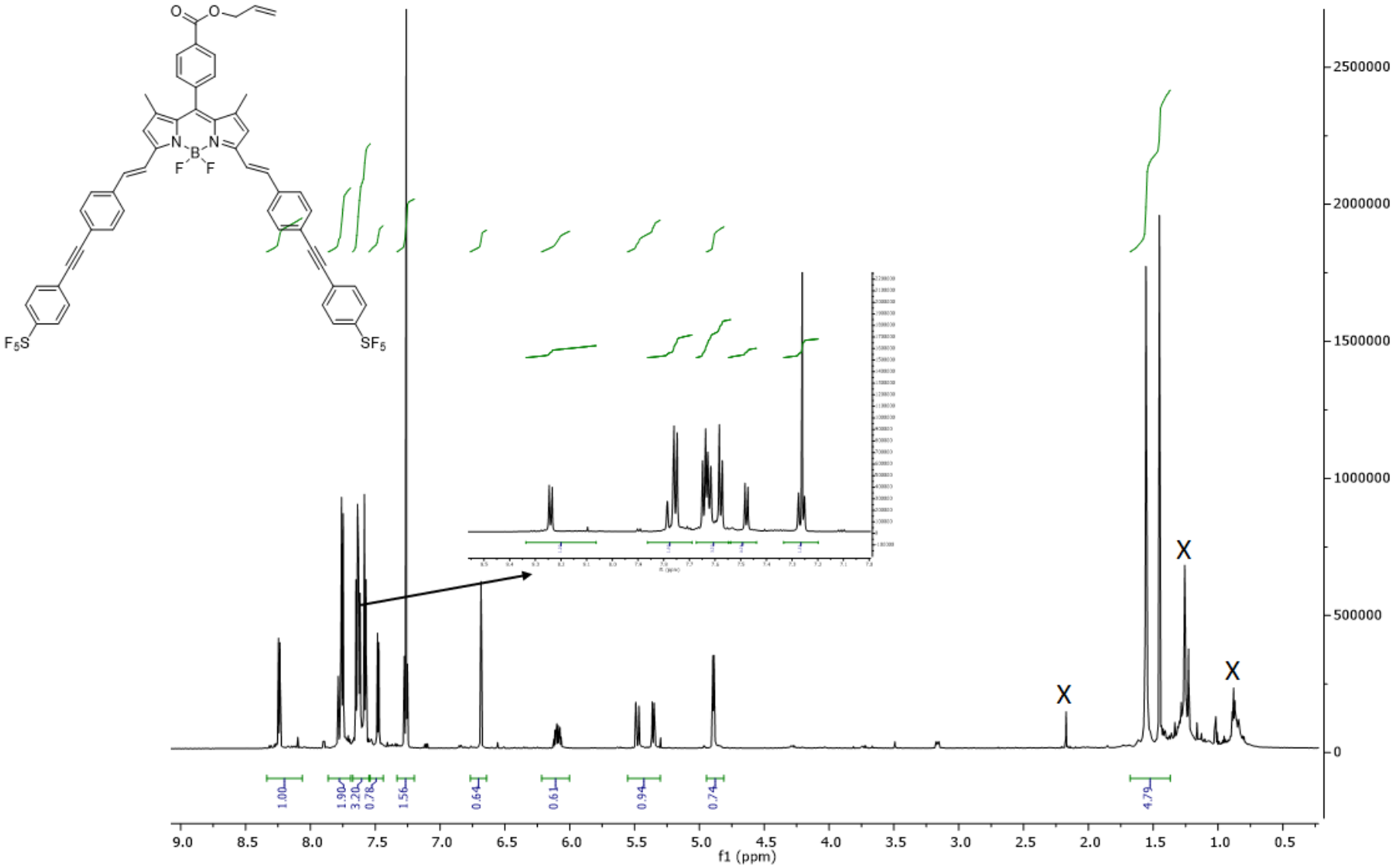

Figure S32. A 700 MHz ^{1}H NMR spectrum of **BD6** recorded in $CDCl_3$. X = trace solvent peaks from acetone and petrol.

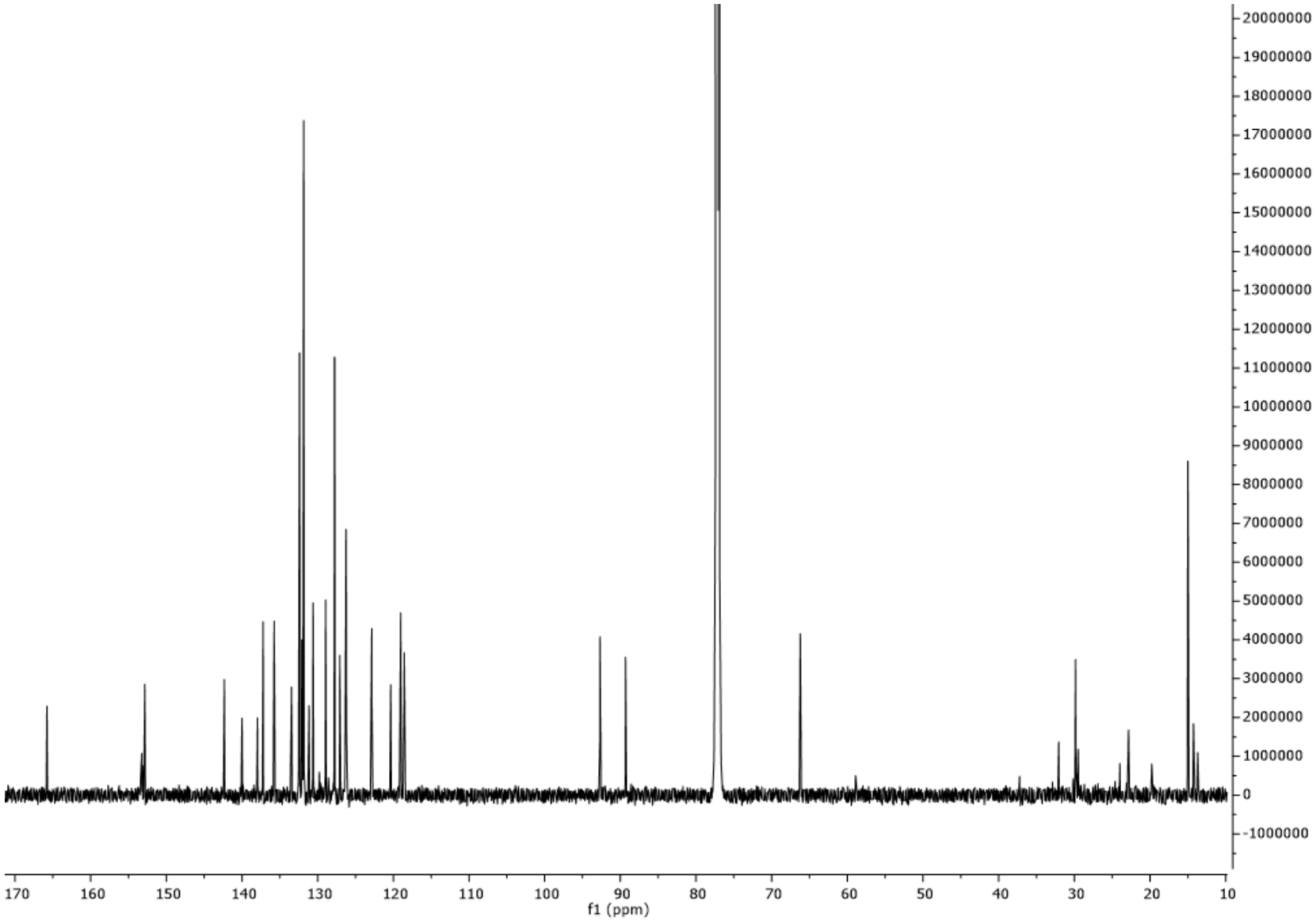

Figure S33. A 176 MHz $^{13}C\{^{1}H\}$ NMR spectrum of **BD6** recorded in $CDCl_3$.

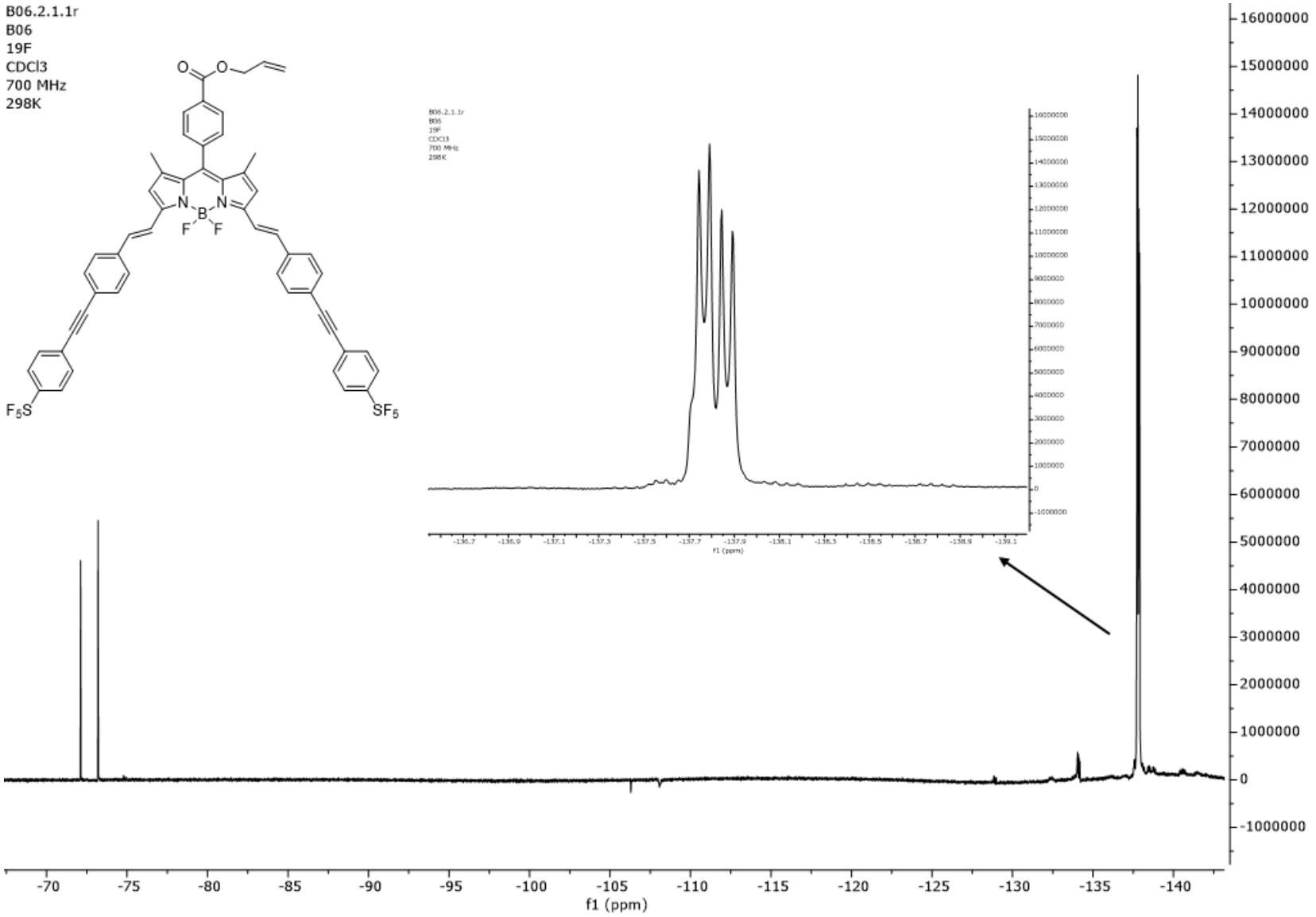

Figure S34. A 659 MHz ^{19}F NMR spectrum of **BD6** recorded in $CDCl_3$.

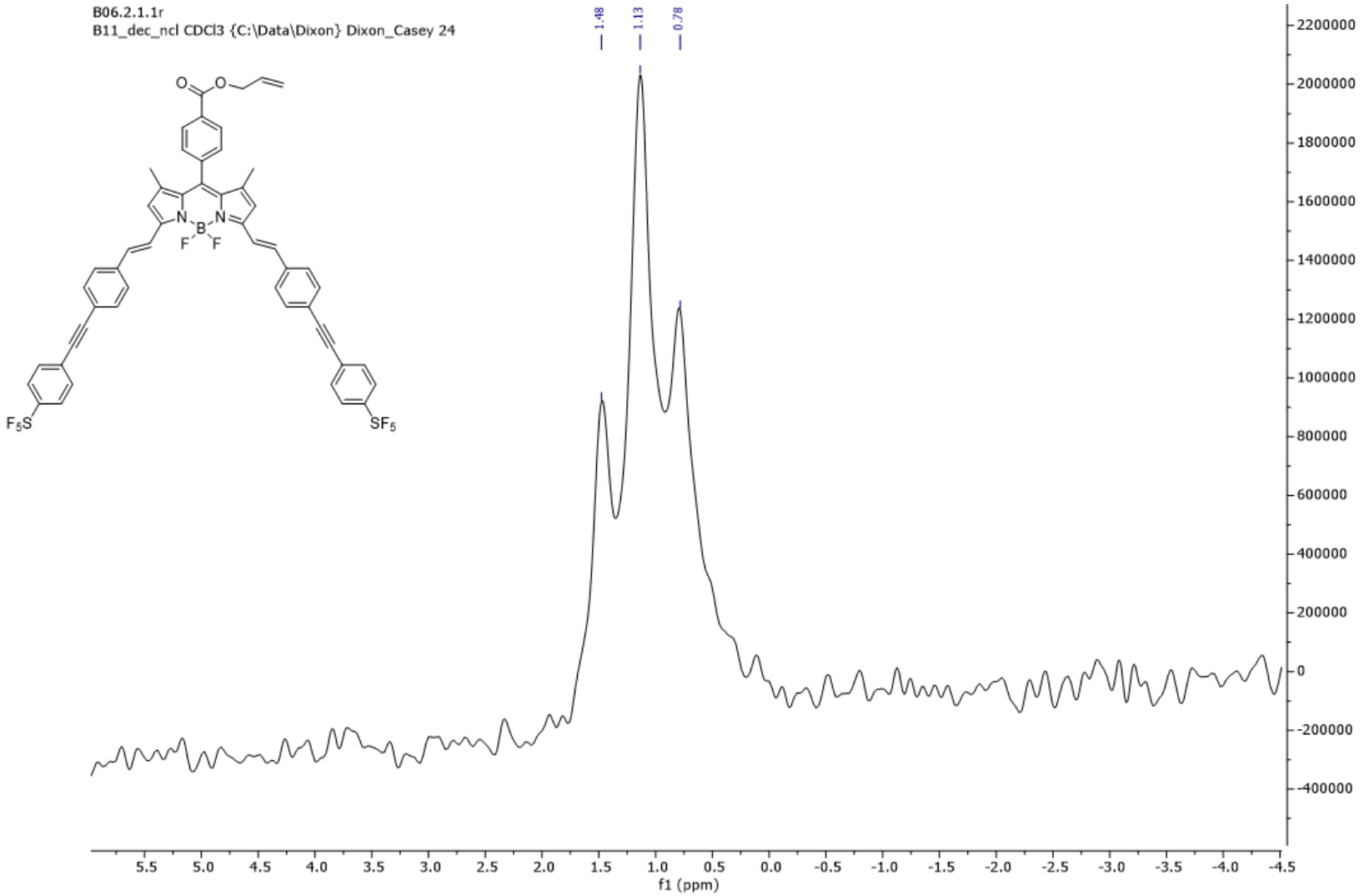

Figure S35. A 96 MHz ^{11}B NMR spectrum of **BD6** recorded in $CDCl_3$.

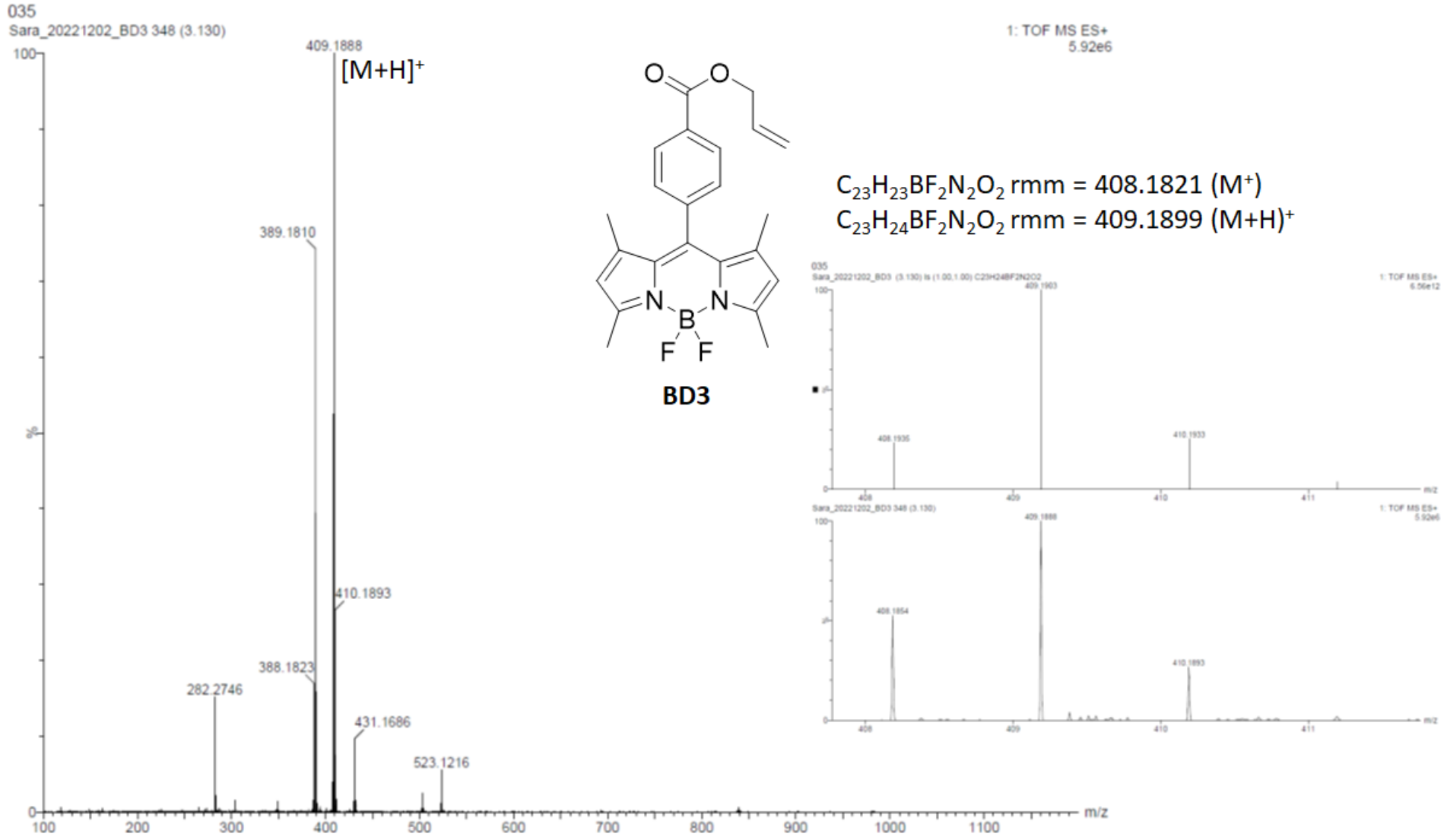

Figure S36. TOF mass spectrum of **BD3** and the comparison of calculated and observed data.

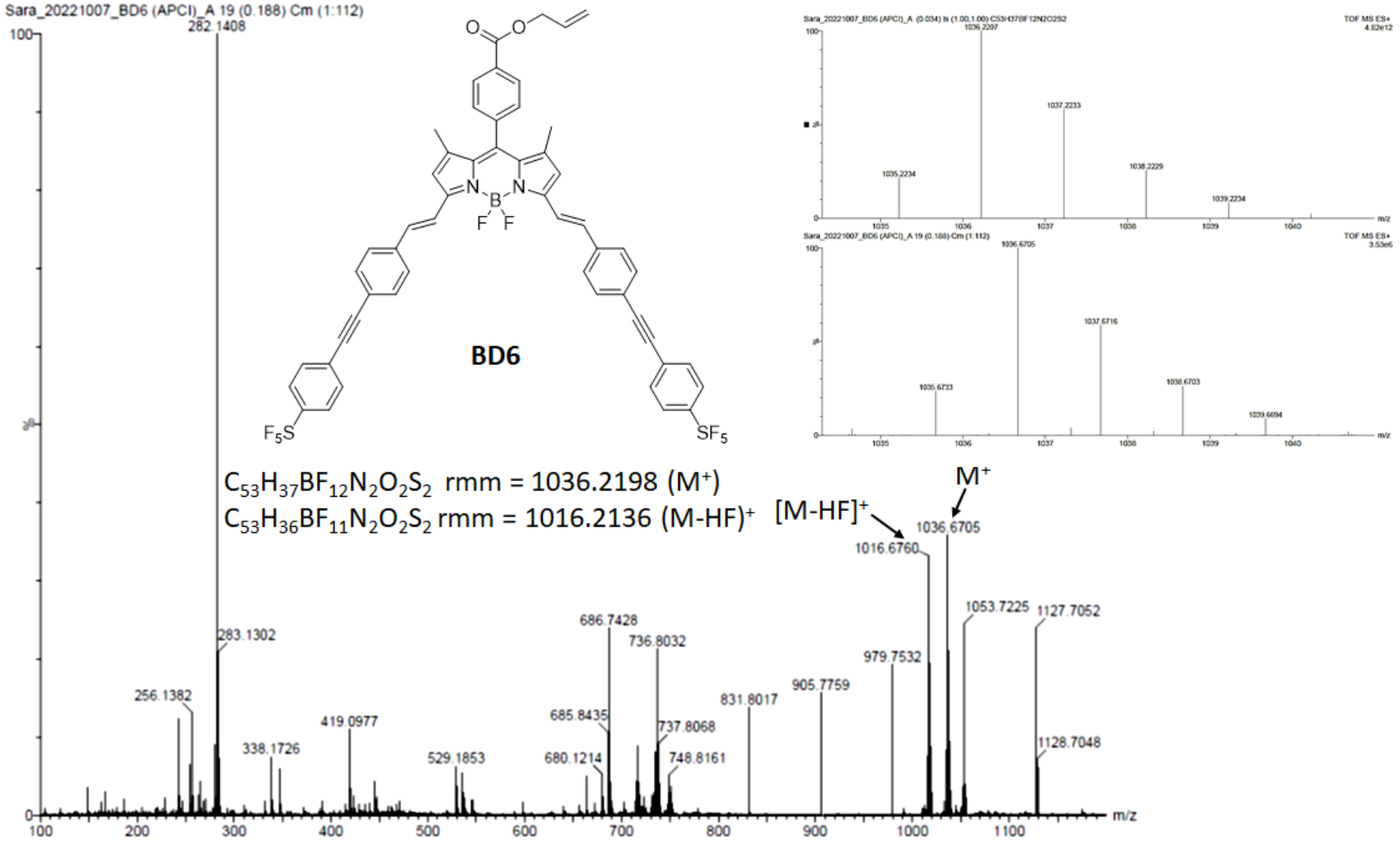

Figure S37. TOF mass spectrum of **BD6** and the comparison of calculated and observed data.